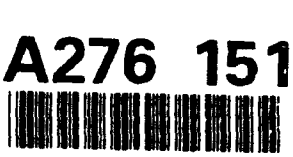

DOT/FAA/CT-93/74
DOT-VNTSC-FAA-93-12

FAA Technical Center
Atlantic City International Airport,
N.J. 08405

A Laboratory Study of Multiple Site Damage in Fuselage Lap Splices

December 1993

Final Report

U.S. Department of Transportation
Federal Aviation Administration

REPORT DOCUMENTATION PAGE

Form Approved
OMB No. 0704-0188

1. AGENCY USE ONLY (Leave blank)	2. REPORT DATE	3. REPORT TYPE AND DATES COVERED
	December 1993	Final Report November 1989-February 1992

4. TITLE AND SUBTITLE
A Laboratory Study of Multiple Site Damage in Fuselage Lap Splices

5. FUNDING NUMBERS
FA3H2/A3128

6. AUTHOR(S)
R. Mayville and M. Sigelmann

7. PERFORMING ORGANIZATION NAME(S) AND ADDRESS(ES)
Arthur D. Little, Inc.*
Acorn Park
Cambridge, MA 02140-2390

8. PERFORMING ORGANIZATION REPORT NUMBER
DOT-VNTSC-FAA-93-12

9. SPONSORING/MONITORING AGENCY NAME(S) AND ADDRESS(ES)
U.S. Department of Transportation
Federal Aviation Administration Technical Center
Atlantic City International Airport, NJ 08405

10. SPONSORING/MONITORING AGENCY REPORT NUMBER
DOT/FAA/CT-93/74

11. SUPPLEMENTARY NOTES
U.S. Department of Transportation
Research and Special Programs Administration
*Under Contract to: Volpe National Transportation Systems Center
Cambridge, MA 02142

12a. DISTRIBUTION/AVAILABILITY STATEMENT
This document is available to the public through the National Technical Information Service, Springfield, VA 22161

12b. DISTRIBUTION CODE

13. ABSTRACT (Maximum 200 words)

This report details an experimental study that was conducted to explore the causes of fuselage lap splice multiple site damage (MSD), which has been observed in several aging aircraft. MSD was partially responsible for the 1988 Aloha Airlines accident. A specimen was designed and tests were conducted to investigate the effects on MSD and fatigue of: (1) a terminating action repair; (2) simultaneous tension and shear; and (3) stress and several lap splice configurations. The results of over 120 tests were supported by finite element analysis, strain gage studies and statistics.

14. SUBJECT TERMS
fatigue, life, fuselage lap, biaxial stress, bucktail diameter

15. NUMBER OF PAGES
118

16. PRICE CODE

17. SECURITY CLASSIFICATION OF REPORT	18. SECURITY CLASSIFICATION OF THIS PAGE	19. SECURITY CLASSIFICATION OF ABSTRACT	20. LIMITATION OF ABSTRACT
Unclassified	Unclassified	Unclassified	

PREFACE

This report details an experimental study that was conducted to explore the causes of fuselage lap splice multiple site damage (MSD), which has been observed in several aging aircraft. MSD was partially reponsible for the 1988 Aloha Airlines accident. A specimen was designed and tests were conducted to investigate the effects of MSD and fatigue of: (1) a terminating action repair; (2) simultaneous tension and shear; and (3) stress and several lap splice configurations. The results of over 120 tests were supported by finite element analysis, strain gage studies and statistics.

This report was prepared for the Volpe National Transportation Systems Center in support of the U.S. Department of Transportation, Federal Aviation Administration. The authors wish to acknowledge Dr. Kemal Arin, Technical Task Initiator, for valuable input in conducting this study.

METRIC/ENGLISH CONVERSION FACTORS

ENGLISH TO METRIC

LENGTH (APPROXIMATE)

1 inch (in) = 2.5 centimeters (cm)
1 foot (ft) = 30 centimeters (cm)
1 yard (yd) = 0.9 meter (m)
1 mile (mi) = 1.6 kilometers (km)

AREA (APPROXIMATE)

1 square inch (sq in, in^2) = 6.5 square centimeters (cm^2)
1 square foot (sq ft, ft^2) = 0.09 square meter (m_2)
1 square yard (sq yd, yd^2) = 0.8 square meter (m^2)
1 square mile (sq mi, mi^2) = 2.6 square kilometers (km^2)
1 acre = 0.4 hectares (he) = 4,000 square meters (m^2)

MASS - WEIGHT (APPROXIMATE)

1 ounce (oz) = 28 grams (gr)
1 pound (lb) = .45 kilogram (kg)
1 short ton = 2,000 pounds (lb) = 0.9 tonne (t)

VOLUME (APPROXIMATE)

1 teaspoon (tsp) = 5 milliliters (ml)
1 tablespoon (tbsp) = 15 milliliters (ml)
1 fluid ounce (fl oz) = 30 milliliters (ml)
1 cup (c) = 0.24 liter (l)
1 pint (pt) = 0.47 liter (l)
1 quart (qt) = 0.96 liter (l)
1 gallon (gal) = 3.8 liters (l)
1 cubic foot (cu ft, ft^3) = 0.03 cubic meter (m^3)
1 cubic yard (cu yd, yd^3) = 0.76 cubic meter (m^3)

TEMPERATURE (EXACT)

[(x-32)(5/9)] ^oF = y ^oC

METRIC TO ENGLISH

LENGTH (APPROXIMATE)

1 millimeter (mm) = 0.04 inch (in)
1 centimeter (cm) = 0.4 inch (in)
1 meter (m) = 3.3 feet (ft)
1 meter (m) = 1.1 yards (yd)
1 kilometer (km) = 0.6 mile (mi)

AREA (APPROXIMATE)

1 square centimeter (cm^2) = 0.16 square inch (sq in, in^2)
1 square meter (m^2) = 1.2 square yeards (sq yd, yd^2)
1 square kilometer (km^2) = 0.4 square mile (sq mi, mi^2)
1 hectare (he) = 10,000 square meters (m^2) = 2.5 acres

MASS - WEIGHT (APPROXIMATE)

1 gram (gr) = 0.036 ounce (oz)
1 kilogram (kg) = 2.2 pounds (lb)
1 tonne (t) = 1,000 kilograms (kg) = 1.1 short tons

VOLUME (APPROXIMATE)

1 milliliters (ml) = 0.03 fluid ounce (fl oz)
1 liter (l) = 2.1 pints (pt)
1 liter (l) = 1.06 quarts (qt)
1 liter (l) = 0.26 gallon (gal)
1 cubic meter (m^3) = 36 cubic feet (cu ft, ft^3)
1 cubic meter (m^3) = 1.3 cubic yards (cu yd, yd^3)

TEMPERATURE (EXACT)

[(9/5) y + 32] ^oC = x ^oF

QUICK INCH-CENTIMETER LENGTH CONVERSION

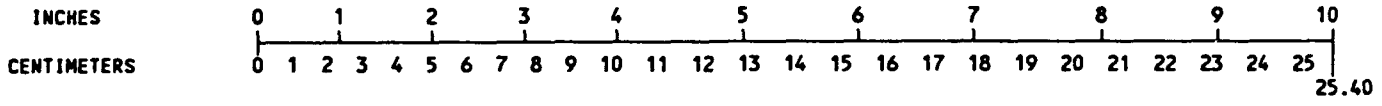

QUICK FAHRENHEIT-CELSIUS TEMPERATURE CONVERSION

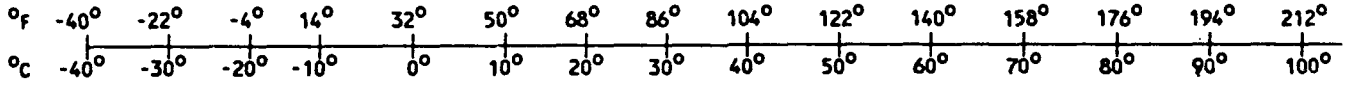

For more exact and or other conversion factors, see NBS Miscellaneous Publication 286, Units of Weights and Measures. Price $2.50. SD Catalog No. C13 10286.

TABLE OF CONTENTS

Section	Page
EXECUTIVE SUMMARY	ix
Introduction	1
Objective and Approach	4
Background	5
Test Specimen and Fixture	9
Baseline Testing	18
Series I Testing: Study of the Terminating Action	22
Test Procedure	23
Series II Testing: The Effects of Superimposed Shear	26
Series III Testing: Study of the Effects of Lap Splice Parameters on Fatigue	32
Series IIIA	32
Experimental Design Considerations	34
Measurements (Definition of Response Variables)	39
Statistical Analysis of Fatigue Life Data	42
Statistical Analysis of MSD Data	48
Series IIIB	53
Discussion	55
Lap Splice Simulation	55
Terminating Action	56
Shear	58
Lap Splice Parameters	59
Conclusions	60
Acknowledgement	63
References	65
Appendix A - MSD Patterns from Selected Specimens	67
Appendix B - Experiments to Determine the Effect of Bucktail Diameter on Fatigue	77
Appendix C - Series III Test Data	83
Appendix D - Definition of MSD	97
Appendix E - Strain Gage Tests on Bending in 12-Inch Wide Panels	103

LIST OF FIGURES

Figure		Page
1.	MSD Observed in the Aloha Aircraft that Experienced a Rapid Decompression	2
2.	An Illustration of a Flush Head Rivet Cross Section, Showing the Knife Edge	3
3.	Photograph of Lap Splice MSD in the Top Row of Rivets from a B727 with 43,433 Flights	6
4.	A Quantitative Description of the MSD from a B727, Part of Which was Shown in Figure 3	7
5.	Angled MSD from a B727 with 42,902 Flights	8
6.	The Geometry of the Panel Used for Most of the Tests in this Study	10
7.	A Photograph of the Test Panel and Fixture	11
8.	An Illustration of the Method Used for Achieving Combined Tension and Shear Loading	13
9.	Stress Distributions in the 12-inch Wide Panel and in a Fuselage	15
10.	An Example of the Crack Pattern from a 12-inch Wide Panel Specimen	16
11.	Comparison of Crack Growth Rates from 12-inch Wide Panels and a Fuselage MSD Crack	17
12.	Comparison of Rivet Cross Sections from Two Panel Batches with Different Amounts of Rivet Deformation; Top - Batch 1; Bottom - Batch 2	21
13.	Comparison of Crack Growth Rates for a Baseline Test and for Terminating Action Tests	24
14.	Results from all of the Baseline Tests	29
15.	An Example of the Cracking Pattern for a Panel Tested at a Shear-to-Tension Ratio of 0.2	30

LIST OF FIGURES (continued)

Figure		Page
16.	The Crack Pattern from one of the Shear/Tension Tests	31
17.	Cross Section of a Briles Rivet in 0.040 inch Thick Sheets	33
18.	The Geometry of the Staggered Rivet Orientation Tested (top) Compared to a Sample from a B727 Fuselage (bottom)	35
19.	An Example of the Fit of Data from Series IIIA to a Weibull Curve	41
20.	Summary of the Series IIIA Data used in the Statistical Analysis	43
21.	An Example of the Output from SAS for Rivet Type	47
22.	Summary of Statistical Analysis for Series IIIA MSD Data	50
23.	The Distribution of Number of Cracks in Series IIIA Panels	52
24.	Data Suggesting that there is a Size Effect on Fatigue Life in Test Panels	57
25.	Cross Section of a Flush Head Rivet in 0.080 inch Thick Sheet	61

LIST OF TABLES

Tables		Page
1.	Materials of Panel Construction	12
2.	Room Temperature Tensile Properties of the 2024-T3 Sheet	14
3.	Baseline Panel Configuration	18
4.	Baseline Fatigue Test Results; Maximum Stress = 16ksi	19
5.	Comparison of Bucktail Diameter and Fatigue Lives for the Baseline Tests	22
6.	Terminating Action Data; Maximum Nominal Stress = 16ksi (R=0.1); Tension Only	25
7.	Shear/Tension Terminating Action Data; Maximum Axial Stress = 16ksi (R=0.1)	27
8.	Fatigue Data for Combined Tension and Shear Loading; Maximum Nominal Stress = 16ksi; R=0.1 Baseline Configuration	28
9.	Parameters Investigated in the Statistically Designed Test Matrix	34
10.	The 27 Combinations of Parameters Tested in Series IIIA	38
11.	An Example of the Effect of One Parameter	44
12.	ANOVA Table - Fatigue Life	45
13.	Summary of Series IIIA Test Results: Fatigue Life	49
14.	Summary of Series IIIA Statistical Analysis Results: MSD (Flush head rivets only)	51
15.	Series IIIB Test Parameters	53
16.	Summary of Series IIIB Test Results - Fatigue Life	54
17.	Summary of Series IIIB Test Results: MSD	54

Executive Summary

An experimental study was conducted to explore the causes of multiple site damage (MSD), which has been observed in several aging aircraft and was partially responsible for the 1988 Aloha Airlines accident. The program had three specific objectives: (1) establish the effectiveness of the terminating action defined by Boeing's Service Bulletin 737-53-1039; (2) determine the effect of shear on lap splice fatigue behavior, and; (3) determine the effect that various lap splice geometric parameters have on fatigue life and MSD.

As part of the project a flat, 12 inch wide, edge-reinforced test panel was developed to simulate a fuselage lap splice. The stress distribution in the test panel was determined through finite element analysis and strain gage tests to have approximately the same membrane stress distribution between tear straps as in a fuselage. Crack growth rates and MSD patterns in the test panel were also very similar to those observed from a few samples taken from aircraft. However, it appears that the panel fatigue life may be a factor of two greater than the fuselage counterpart based on available data.

Tests were performed to simulate application of the terminating action to uncycled and precycled lap splices. Results indicate that the replacement of flush head rivets with protruding head rivets in enlarged holes results in at least a four- to five-fold increase in fatigue life. Elimination of the knife edge does not fully explain the difference in fatigue life. This was demonstrated by comparable improvements in life even when cracks beyond the protruding head rivet hole were purposely introduced. The terminating action was found to be equally effective when combined shear and tension were applied.

The application of shear with tension to simulate conditions at the window line caused a 33% reduction in fatigue life in the baseline flush head rivet configuration, but no perceptible difference in MSD formation. Such a reduction is difficult to explain only by the minor increase in principal stress due to the addition of shear.

The majority of the testing in this study was directed toward the investigation of the effect that lap splice parameters have on fatigue life and MSD. Two series of tests were conducted. In the first, six different parameters, each varied over two or three test levels, were evaluated to establish which have a dominant effect. A second series was then conducted to investigate the behavior of the most significant of these parameters when varied over a wider range of test conditions. Parameters studied included: stress level, rivet type (including Briles rivets), rivet spacing, rivet orientation, number of rivet rows and skin thickness.

Definitions of fatigue life and MSD were required for this study. Fatigue life, or fatigue initiation, was defined as the number of cycles required to grow the first crack in the top row of rivets to 0.1 inches. Although considerable research is now underway to improve inspection methods, 0.1 inches has often been cited as the minimum crack size that can be detected reliably in regular structural inspections. A definition for MSD was derived to provide an index from 0 to 1. A value of zero corresponds to the total absence of cracks, while a value of 1 corresponds to uniform MSD, that is, equal size cracks emanating from each side of each rivet hole, with a size that would satisfy the net section yield criterion. MSD in a B727 lap splice example was equal to 0.28 by this definition.

Statistical experimental design concepts were used to reduce the number of configurations required for testing in the first series; duplicate tests were also performed in most cases. The results showed that only stress level, rivet type and skin thickness had a statistically significant effect on fatigue lives; other parameters showed trends, but more tests would be required to assure that the differences observed in this program are reproducible. As expected, higher stresses caused lower lives and the Briles rivet was found to provide significantly longer fatigue lives relative to flush head rivets. Curiously, no obvious trend with skin thickness was detected. None of the parameters tested in the first series had a significant effect on MSD, although a clear trend of increasing MSD with higher stress was evident. However, MSD occurred in just about every flush head rivet configuration tested.

Additional stress and skin thickness levels were selected for testing in the second series because of the observed dominant effect of the former and the practical importance of the latter; higher skin thicknesses are often cited as improving fatigue performance because of elimination of the knife edge. These additional tests confirmed the finding that higher stress levels dramatically decreased fatigue life and also increased the propensity toward uniform MSD. Greater thicknesses were also found to significantly increase fatigue life; however, the increase was less than a factor of two in going from a thickness of 0.040 to 0.080 inches.

Introduction

In 1988 the Federal Aviation Administration initiated a substantial research program to better understand the issues related to the aging commercial aircraft fleet. A motivating factor for this research was the Aloha Airlines accident in which a portion of the fuselage tore away from an aircraft in flight. The National Transportation Safety Board investigated several causes for the accident [1]. One of these is a phenomenon commonly referred to as multiple site damage or MSD.

Multiple site damage found in the failed aircraft was located along lap splices joining sections of skin in the fuselage. It consisted of several small cracks in adjacent holes in the top row of rivets, Figure 1. Failure of the adhesive bond at the joint together with several pressurization cycles - 89,000 in the case of the Aloha aircraft - resulted in earlier than expected fatigue at the lap splice joint. The knife edge associated with the thin skin, as illustrated in Figure 2, was also felt to contribute to the relatively low fatigue life.

An inspection schedule and repair had been generated and published by Boeing as early as 1972 for several of the lap splices in the most heavily used, early B-727 and B-737 aircraft [2]. The repair consists of removing the top row of flush head rivets in the joints in question, enlarging the holes, inspecting for cracks and, if none are found, installing larger, button head rivets. A substantial gain in fatigue life is then expected, primarily because of the elimination of the sharp knife edge.

This corrective action was generally viewed as sound, but there had been no published studies to support its effectiveness or to ensure that the MSD found in early B-727, 737 and 747 aircraft would not occur in other aging aircraft or at other lap splice details.

This report describes a program initiated by the FAA to investigate the conditions under which lap splice MSD can occur and whether the required repair technique is likely to be effective.

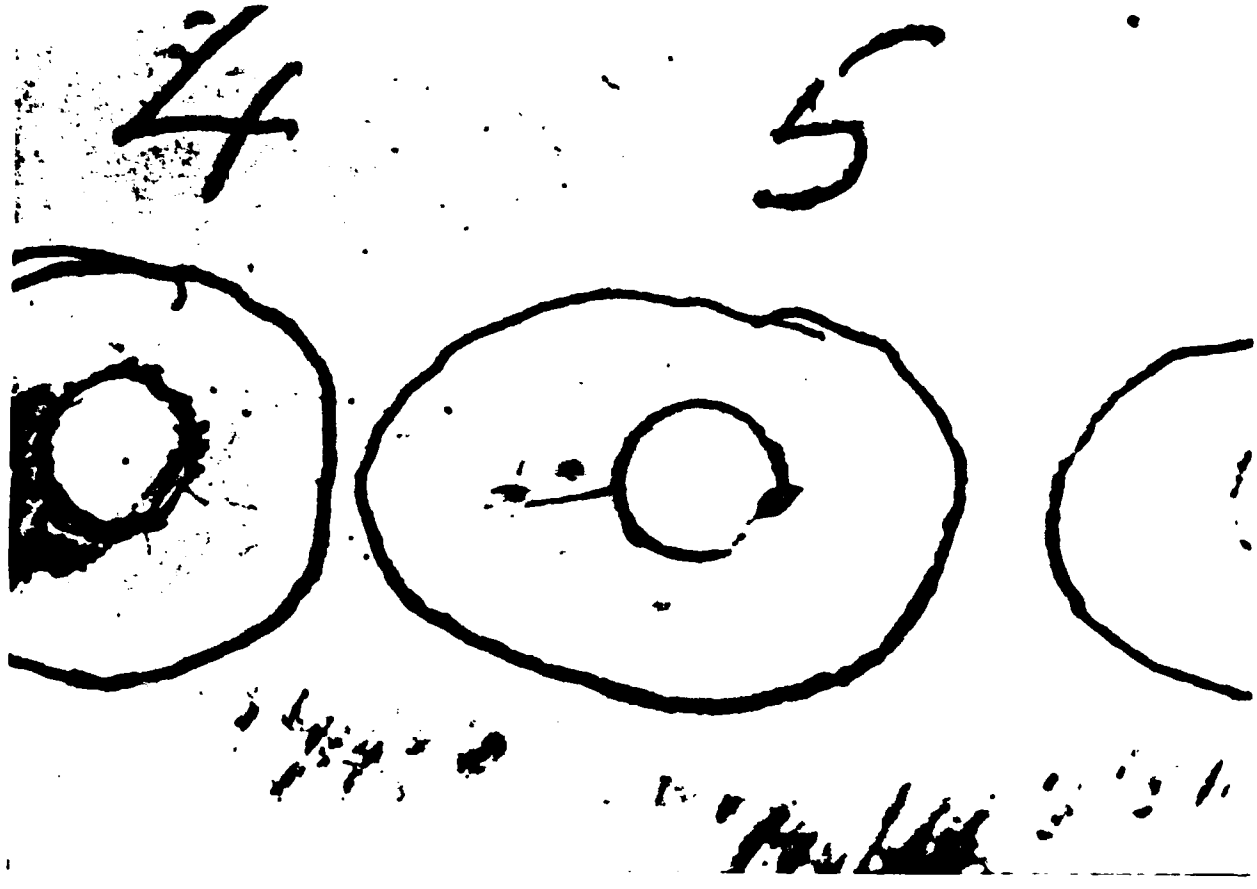

Figure 1: MSD Observed in the Aloha Aircraft that Experienced a Rapid Decompression

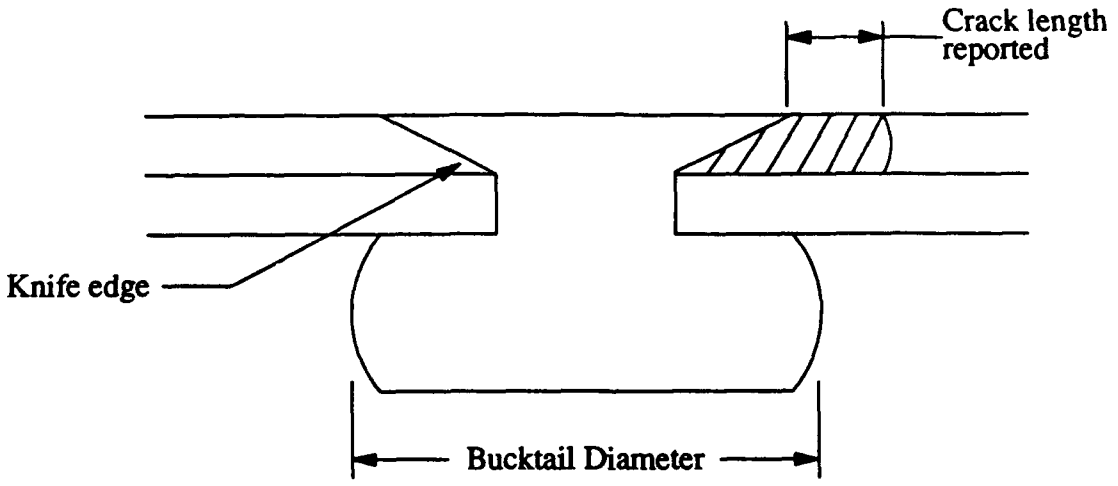

Figure 2: An Illustration of a Flush Head Rivet Cross Section, Showing the Knife Edge

Experiments on over 150 specimens have produced several key results. Simulation of the required repair procedure indicates that installation of the button head rivets is very effective even after the accumulation of substantial fatigue damage. The addition of shear stresses, simulating a lap splice near the window line, was also shown to exacerbate the formation of MSD. A comprehensive study of lap splice geometric parameters suggests that MSD is more severe for higher stresses and can occur in just about any configuration; however, the number of cycles for it to initiate varies over nearly two orders of magnitude. The program that led to these conclusions is described in the pages that follow.

Objective and Approach

The objective of this investigation was to determine the conditions under which lap splice MSD can occur in fuselage lap joints. The concentration was on the formation of cracks, not on the fracture event.

The approach has been largely experimental. A 12 inch wide, flat panel specimen was developed to provide simulation of the mechanical conditions of a fuselage lap splice joint. Fatigue tests were then conducted on a baseline configuration to correlate laboratory fatigue behavior with observations on actual fuselages. This was followed by the performance of three test series: I - investigation of the terminating action repair; II - study of the effects of superimposed shear and; III - investigation of the effects of lap splice parameters on fatigue behavior. The study was supported by metallography, strain gage and finite element stress analysis and statistical experimental design and data analysis.

Background

An understanding of the MSD that has been observed in aircraft is needed for an assessment of the applicability of the panel specimen to simulate fuselage conditions. Multiple site damage generally refers to the formation of several sites of damage in the same structural member that together could weaken the member beyond the level that would be caused by any individual damage alone. Lap splice MSD is referred to here as the occurrence of several cracks emanating from adjacent rivet holes in a longitudinal joint that connects two sheets of skin in the fuselage. This cracking is due to fatigue from the fuselage pressurization cycles corresponding to each fight. Figure 1 showed an example of lap splice MSD, which will be referred to simply as MSD in this report.

A few cases of MSD in actual aircraft have been examined as part of this investigation. Figure 3 shows a photograph of a 0.039 inch thick lap splice section removed from a B727 as part of a repair. This aircraft had experienced 57,988 flight hours and 43,433 flights. Figure 4 shows a quantitative description of this MSD in terms of the length of each of the individual cracks (from the flush head rivet diameter, Figure 2); there are numerous cracks of significant size in this piece.

MSD can occur as either straight or angled cracks. An example of the latter is shown in Figure 5; this piece was removed from a B727 which had experienced 42,902 flight hours and 31,301 flights. Angled cracking is observed at the window belt line and is probably due to the addition of shear stress from down bending of the fuselage during flight. The angle formed by the crack in Figure 5 is approximately 30° to the axis of the fuselage.

Some general observations can be made from these and other examples reported in the literature (c.f. [1,3]). The MSD cracks are nearly always located in the top row of rivets with a greater concentration toward the region between circumferential stiffeners. The top row crack location is due to a combination of two factors: high stress and the

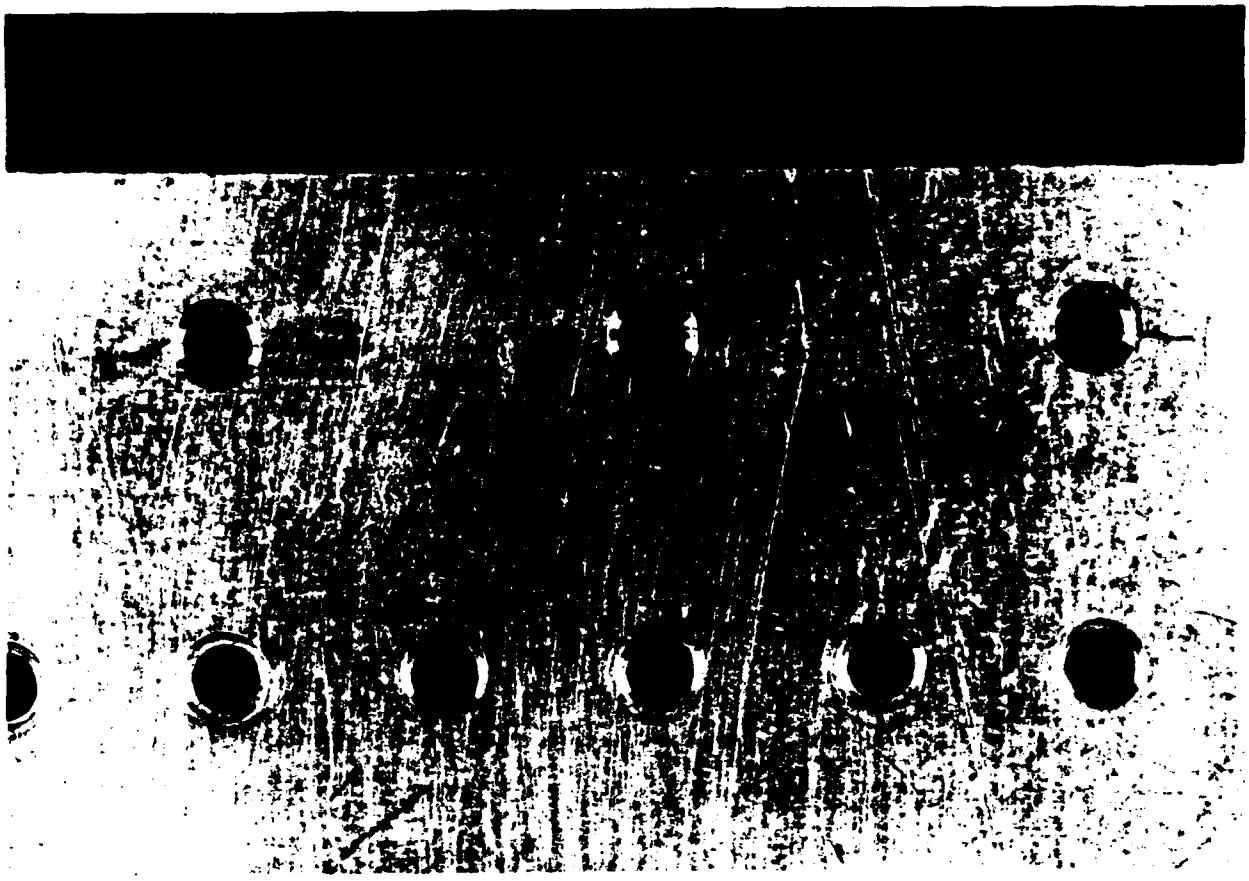

Figure 3: Photograph of Lap Splice MSD in the Top Row of Rivets from a B727 with 43,433 Flights

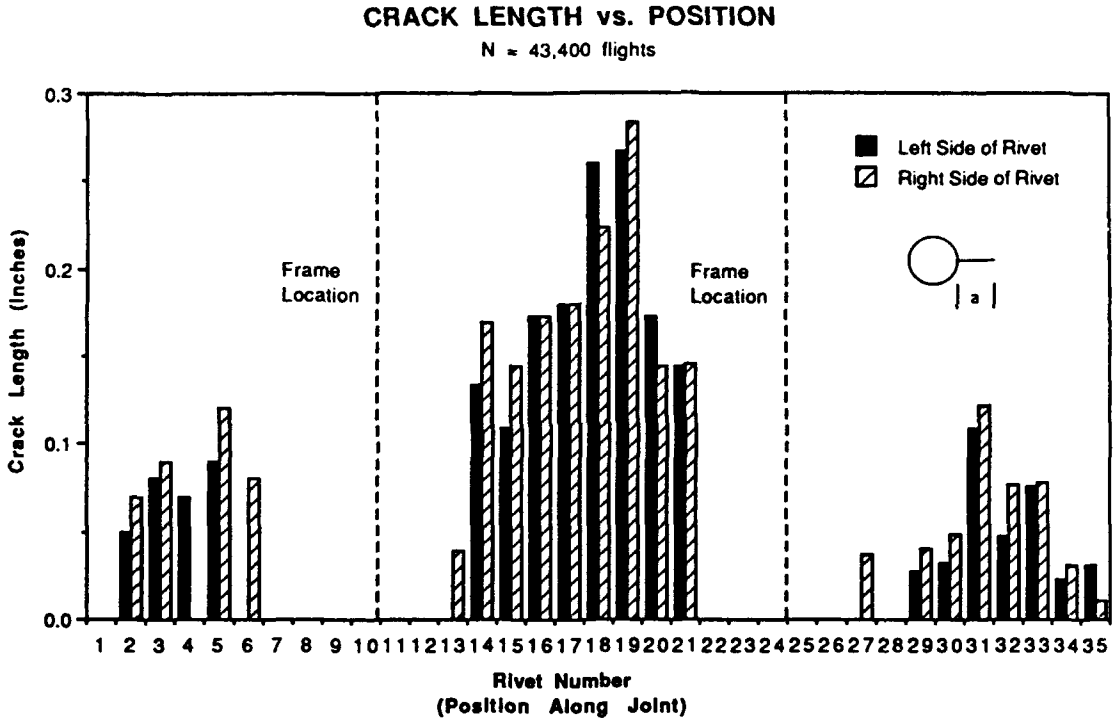

Figure 4: A Quantitative Description of the MSD from a B727, Part of Which was Shown in Figure 3

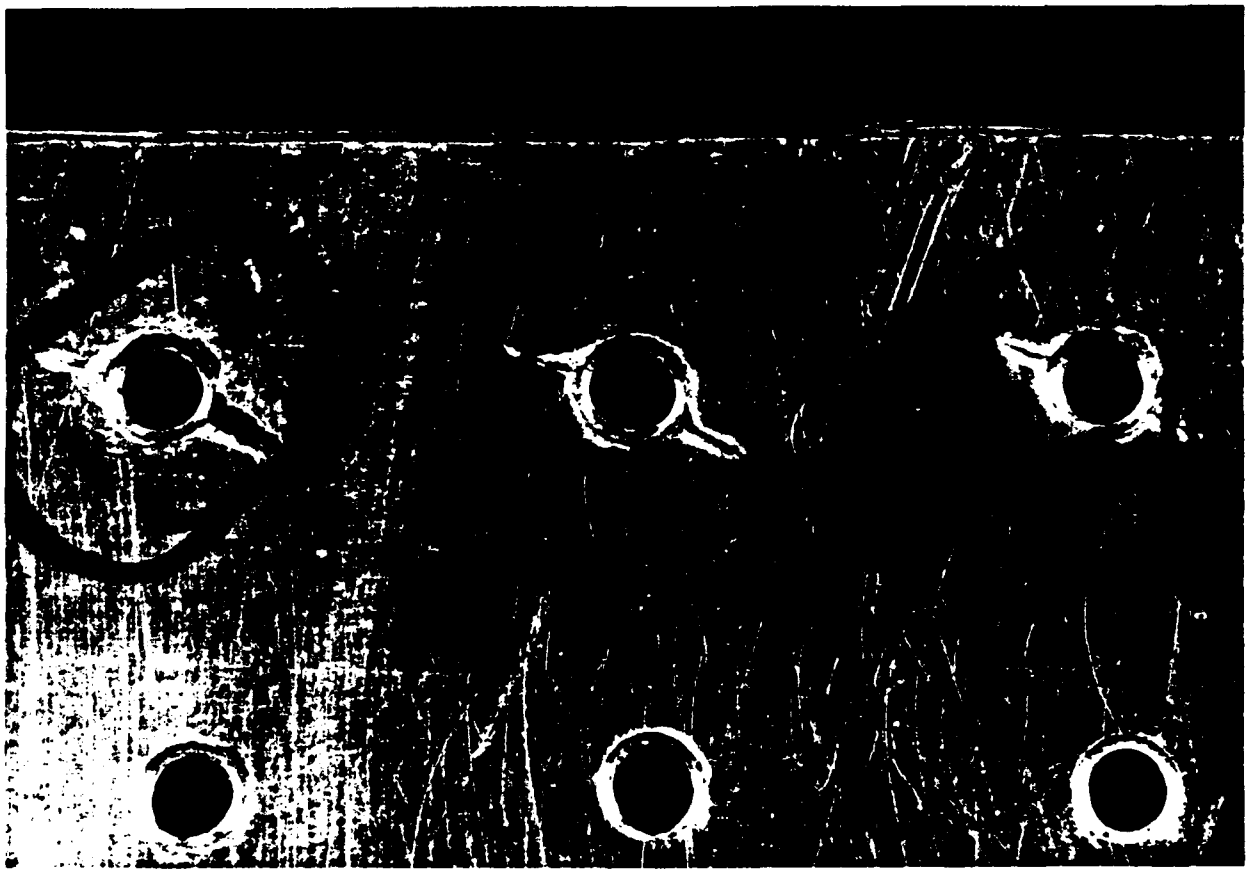

Figure 5: Angled MSD from a B727 with 42,902 Flights

countersink stress concentration. Pressurization of the fuselage causes the greatest stress to occur at the top row in the upper skin and at the bottom row in the lower skin. Because the countersunk holes are machined only in the upper skin, this is the most likely site for initiation of fatigue cracks. Cracks concentrate in between stiffeners because of the reduced skin stress near the frames and tear straps. The striking feature of MSD is the relative uniformity in crack sizes over a given lap splice segment; for example, Figure 4. Another observation about MSD in aircraft, and one we have observed in our laboratory, is the occasional occurrence of cracks in the second row of rivets [1].

Crack growth rates have also been estimated for lap splice MSD. Fractography was conducted on the piece shown in Figure 3 [4] from which analysis of striation spacing indicates that the crack growth rate was relatively constant for extensions up to 0.25 inches and equal to about 6.4×10^{-6} inches/cycle. Striation counting was also conducted on seven MSD cracks from the Aloha Airlines aircraft [1] giving approximate crack growth rates that ranged from $3.5\text{-}6.8 \times 10^{-6}$ inches/cycle.

Test Specimen and Fixture

Design of the test specimen and loading fixture was based on two criteria: reasonable simulation of fuselage stress conditions and relatively low fabrication and testing costs. The initial panel concept was generated as part of another project [5]. Ease of fabrication and testing is best satisfied by a flat panel loaded in tension. The nonuniform membrane stress distribution found in an aircraft is achieved by attaching simulated tear straps to the sheet in approximately the same locations as the tear straps found in some aircraft; that is, on the order of 10 inches apart.

The panel geometry developed in this program is shown in Figures 6 and 7. Total width is 12 inches with two inch wide, 10 inch long tear strap reinforcements fastened at the edges with rivets; this results in a 10 inch spacing between the centers of the reinforcements. The tear straps are attached to the upper and lower sheets with button

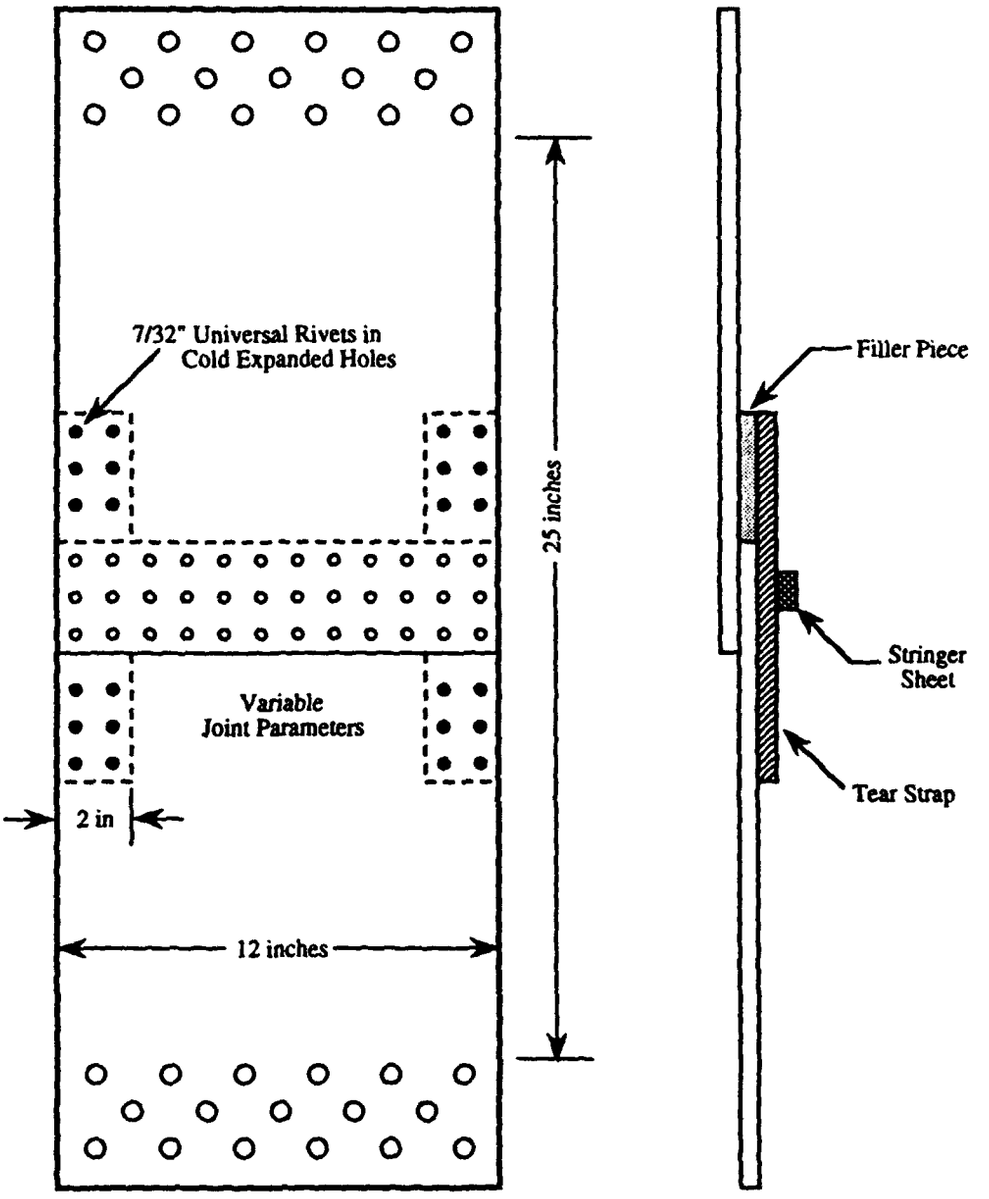

Figure 6: The Geometry of the Panel Used for Most of the Tests in this Study

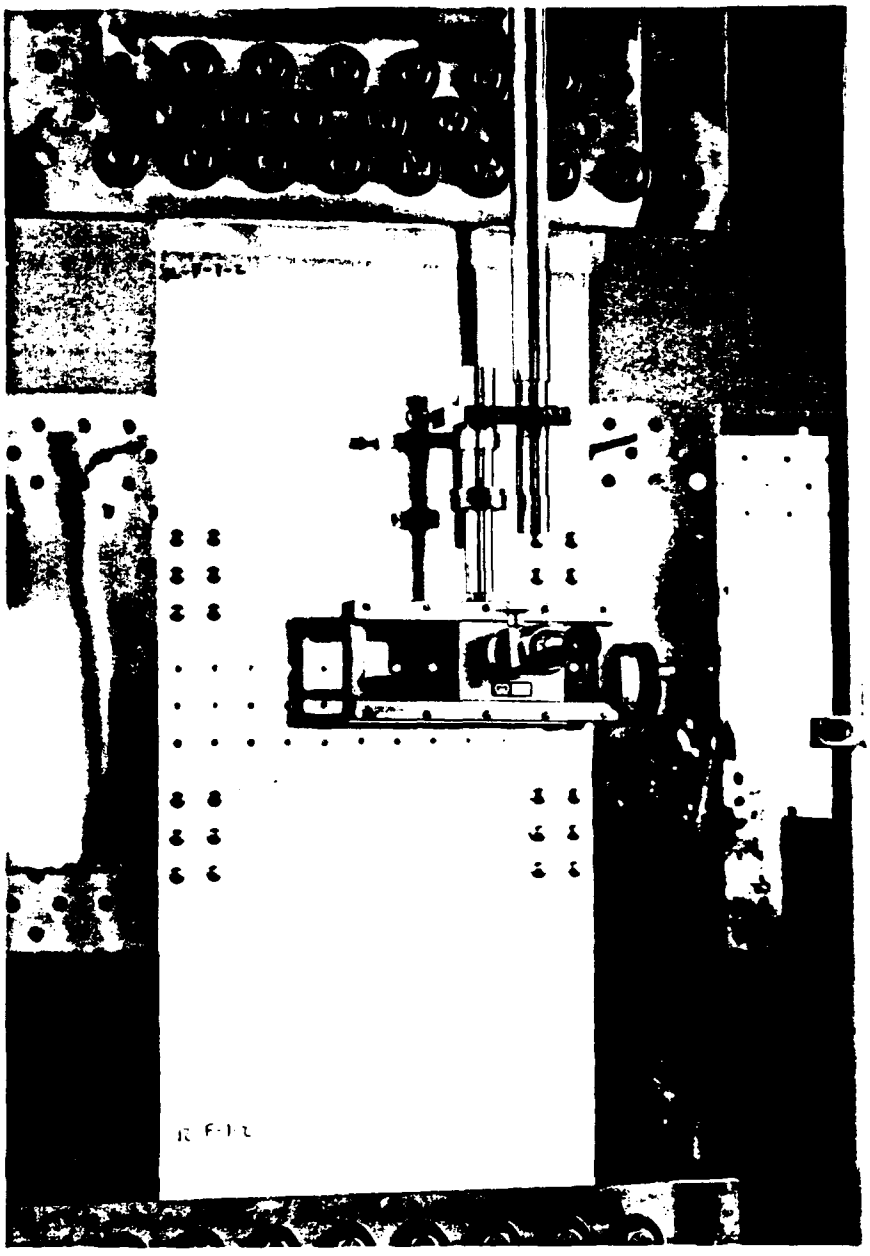

Figure 7: A Photograph of the Test Panel and Fixture

head rivets installed in cold expanded holes. This method of construction was found to be necessary after cracking initiated at the top rivets in the reinforcements at low lives. Figure 6 shows the baseline lap splice geometry; several other geometries were also tested. The lap did not include a bond or a coating in order to simulate the most severe rivet loading condition. A strip of one inch wide sheet was included along the center row of rivets on the rear of the lap splice to represent the thickness of a stringer; this was included to help simulate the lap splice rivet conditions. Rivets were installed according to Specification BAC 5004.

Table 1 lists the materials and the various rivet types used. The rolling direction of the sheet was transverse to the axis of the specimen in all cases. Table 2 shows the room temperature tensile properties from 0.040 inch thick sheet.

Load is applied to the specimen through a bolted plate arrangement at each end of the specimen, Figure 7. A laminate material is sandwiched between the steel plates and the aluminum specimen to prevent fretting fatigue. The steel plates are attached to the testing machine through pinned connections. Simultaneous application of shear is achieved by loading the grips off-axis as illustrated in Figure 8. The fixture is capable of applying shear/tension ratios up to 0.2.

Table 1: Materials of Panel Construction

Sheet (skin):	2024-T3 clad aluminum
Flush head rivets:	2017-T4 aluminum; anodized; 100° shear head (BACR15CE5D)
Protruding (button) head rivets:	2117-T31 aluminum; anodized, close tolerance shank (MS20470AD7)
Briles rivets:	7050-T73 aluminum; anodized; 120° head (BRFZ5E)

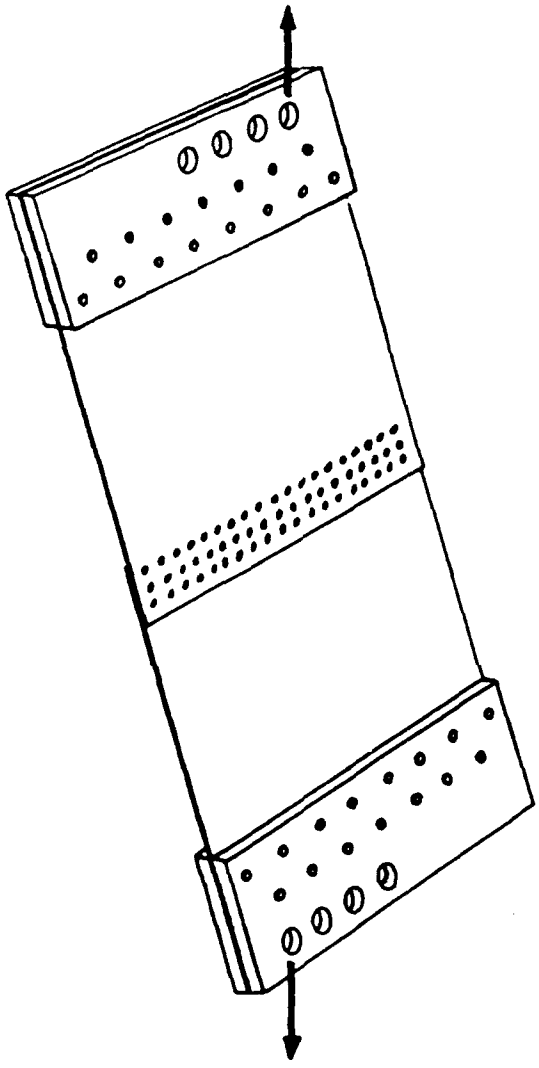

Figure 8: An Illustration of the Method Used for Achieving Combined Tension and Shear Loading

Table 2: Room Temperature Tensile Properties of the 2024-T3 Sheet; (average of two specimens)

	Yield* (ksi)	Tensile (ksi)	Elongation (% in 2 inches)
Longitudinal	44.7	63.0	14.0
Transverse	39.0	58.0	16.5

*0.2% offset

The stress distribution in the test panel was determined with finite element analysis and strain gages. The finite element analysis modeled the thickness of the various structural elements in the panel and the individual rivets but did not include the offset in midplanes of the upper and lower sheets; that is, bending was not modeled. Strain gages were applied on both sides of the upper sheet at four locations along the lap splice, one inch above the top row of rivets.

The results of the finite element and strain gage analyses for membrane stress are plotted in Figure 9 with numerical results for an aircraft fuselage section from [5]. The stress distributions from all three sources are seen to agree quite well; the fuselage finite element results are asymmetric because the spacing between frames is twice as great as the spacing between tear straps.

The crack pattern from one of the baseline tests with this panel design is shown in Figure 10 and is observed to bear a strong resemblance to the crack pattern in Figure 4 corresponding to MSD from an actual aircraft. Figure 11 is a plot of crack length vs. number of cycles for two of the individual cracks from a baseline test which also compare well to the fatigue crack growth measured fractographically for the crack in an actual fuselage.

These results indicate that the 12 inch wide, reinforced, flat panel is providing a reasonable simulation of an aircraft lap splice. One aspect for which the panel may not provide good simulation is in the degree of bending. Although the effect of bending has

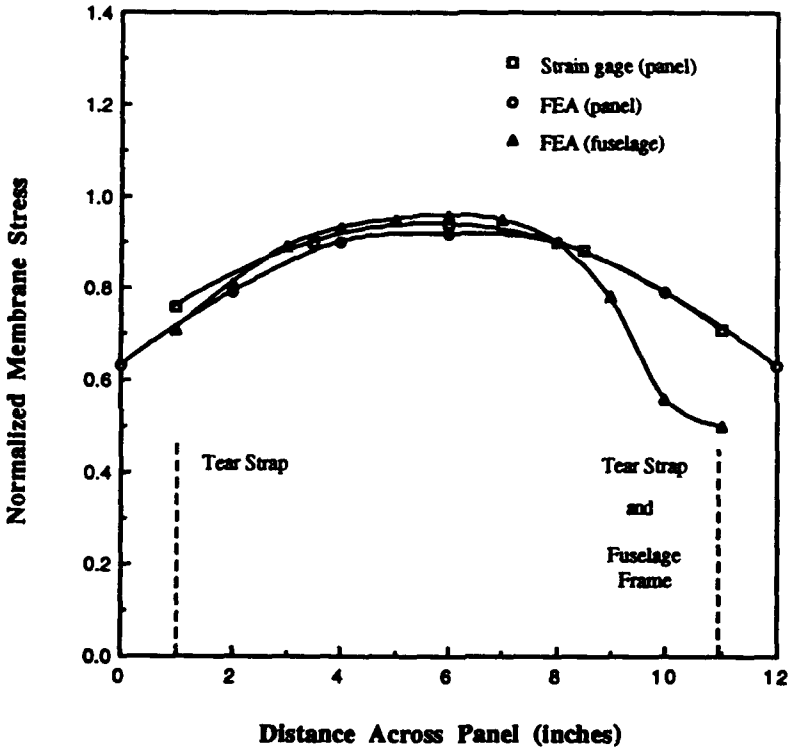

Figure 9: Stress Distributions in the 12 inch Wide Panel and in a Fuselage

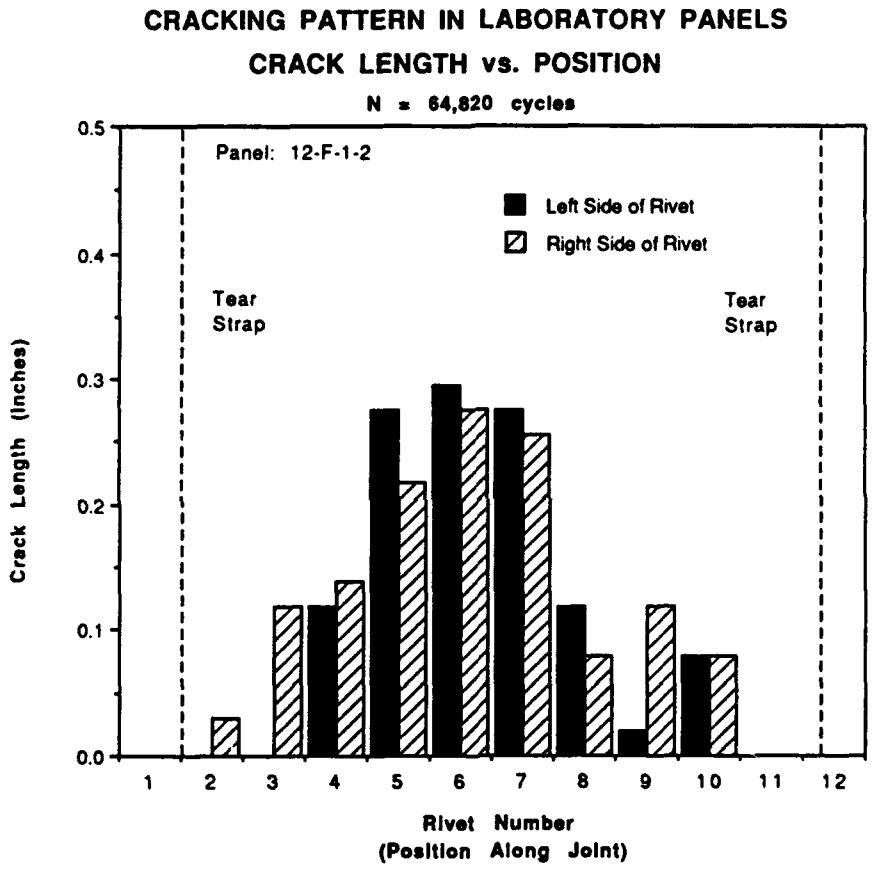

Figure 10: An Example of the Crack Pattern from a 12 inch Wide Panel Specimen

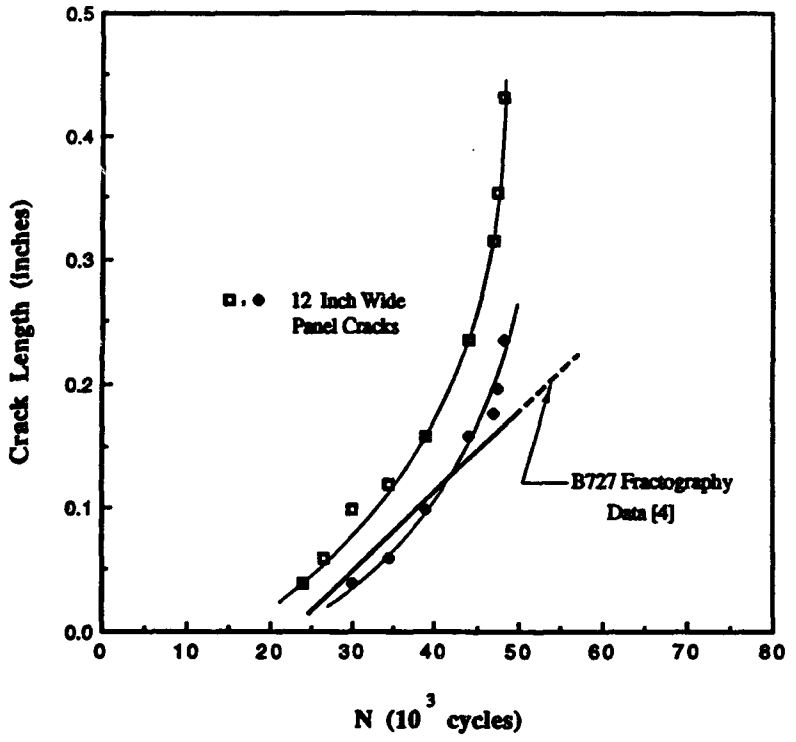

Figure 11: Comparison of Crack Growth Rates from 12 inch Wide Panels and a Fuselage MSD Crack

not been thoroughly investigated, some data are provided later in this report.

Baseline Testing

An initial set of experiments was performed to establish a baseline from which comparison of the effects of various parameters could be made. The lap splice geometry for the baseline configuration is listed in Table 3. A maximum nominal stress of 16ksi was applied as representative of some fuselages.

Table 3: Baseline Panel Configuration

Skin thickness:	0.040 inches
Rivet type:	Flush head, 100° taper, 0.156 inch shank diameter
Rivet spacing:	1 inch
Number of rows:	3
Row spacing:	1 inch

The same procedure for these tests was used throughout this study unless otherwise indicated. Several panel dimensions were recorded prior to testing, including: upper and lower sheet thickness and width; rivet spacing, row spacing and bucktail diameter (top row rivets only); bucktail diameter was defined in Figure 2. Panels were installed in the plate fixtures and the bolts inserted without the application of external load. The bolts were then tightened with only the dead weight load of the bottom grip to ensure that alignment was achieved. All panels strain gaged during this program verified the alignment of the specimens. All fatigue tests, except for a few early tests, were cycled with an R-ratio (ratio of minimum-to-maximum stress) of 0.1. Tests were conducted in load control at a frequency of 4 Hz and the environment was ambient. Nearly all tests were conducted with antibuckling bars. These bars were steel channels whose flanges butted against the lap splice and were loosely bolted together at their ends outside of the 12 inch width section. Pieces of rubber were used to protect the panel from the steel channels.

Crack growth was measured periodically during testing with a traveling, optical microscope. Care was taken to obtain at least two measurements: (1) the number of cycles to grow the first crack to 0.1 inches beyond the rivet head and; (2) the crack length distribution when the first crack reached a length of 0.25 inches. The first measure was chosen as an initiation criterion. It is possible to detect cracks visually on the panels as small as 0.020 inches but a larger size was selected for a few reasons: first, use of a 0.1 inch length makes it much easier to detect the crack without constantly monitoring the test and, second, a crack size of approximately 0.1 inches is apparently the smallest crack size that inspectors in the field have a high chance of detecting during routine inspection [6]. The second measure, 0.25 inches, corresponds approximately to the critical crack size for fracture from uniform lap splice MSD [7]. In many cases, sufficient crack length data were obtained to calculate crack growth rates. (The definition of crack length used in this study was shown in Figure 2.)

The results for two batches of specimen (fabricated at separate times) are shown in Table 4.

Table 4: Baseline Fatigue Test Results;
Maximum Stress = 16ksi

		Number of Cycles to First	
Specimen ID	**R**	**0.1 inch Crack**	**0.25 inch Crack**
Batch 1			
12-F-1-1	0.05	30,000	44,530
12-F-1-2	0.10	50,900	62,710
12-F-1-3	0.10	36,500	49,440
12-F-1-4	0.05	40,000	56,500
12-F-1-5	0.05	82,000	100,000
12-F-1-6	0.05	53,000	71,000
		Avg.= 48,700	
Batch 2			
12-FB-5A1	0.10	96,300	*
12-FB-5A-2	0.10	85,500	*
12-FB-5D-1	0.10	127,300	*
12-FB-5D-2	0.10	76,400	*
		Avg.= 96,400	

* These specimens were subsequently used for terminating action tests

The results from some of these tests have already been presented in the previous section to show that the panel provides some simulation of the fuselage lap splice. Figure 10 showed an example of the crack pattern that developed in one of these panels and is typical of other patterns from these two batches; Appendix A shows some other examples. Likewise, Figure 11 showed how the crack growth rate from a baseline laboratory test compared favorably to that in an example of fuselage MSD.

Some other interesting results emerged from these baseline tests. Cycles to crack initiation varied from 30,000 to 127,000. Although it is not possible to relate these lives to those in aircraft, for which, among other things, the number of flights beyond a no-bond condition is unknown, the range correlates reasonably well with the limited data we do have: 31,301 and 43,000 flights for the B727 examples referred to earlier and approximately 89,000 for the Aloha aircraft. The data of Table 4 also show a substantial difference in fatigue lives between the two batches: average cycles to 0.1 inch cracking of 48,700 for Batch 1 and 96,400 for Batch 2. This difference was due to variation in rivet deformation during installation. Figure 12 shows a magnified cross section of a rivet in the top row from each of the batches. The greater rivet deformation in Batch 2 resulted in a blunting of the knife edge, which is considered to be the primary cause of low fatigue lives in the lap splice joint. Greater rivet deformation is characterized by a larger bucktail diameter. Table 5 compares the average fatigue lives and bucktail diameters for the two batches. While both diameters satisfy specification BAC 5004 the larger diameter is preferred in practice. An auxiliary experimental task was undertaken to better reveal the effect of bucktail diameter on fatigue, the description of which is given in Appendix B. Based on the results described above and in Appendix B, the bucktail diameter was controlled very carefully in all subsequently fabricated panels.

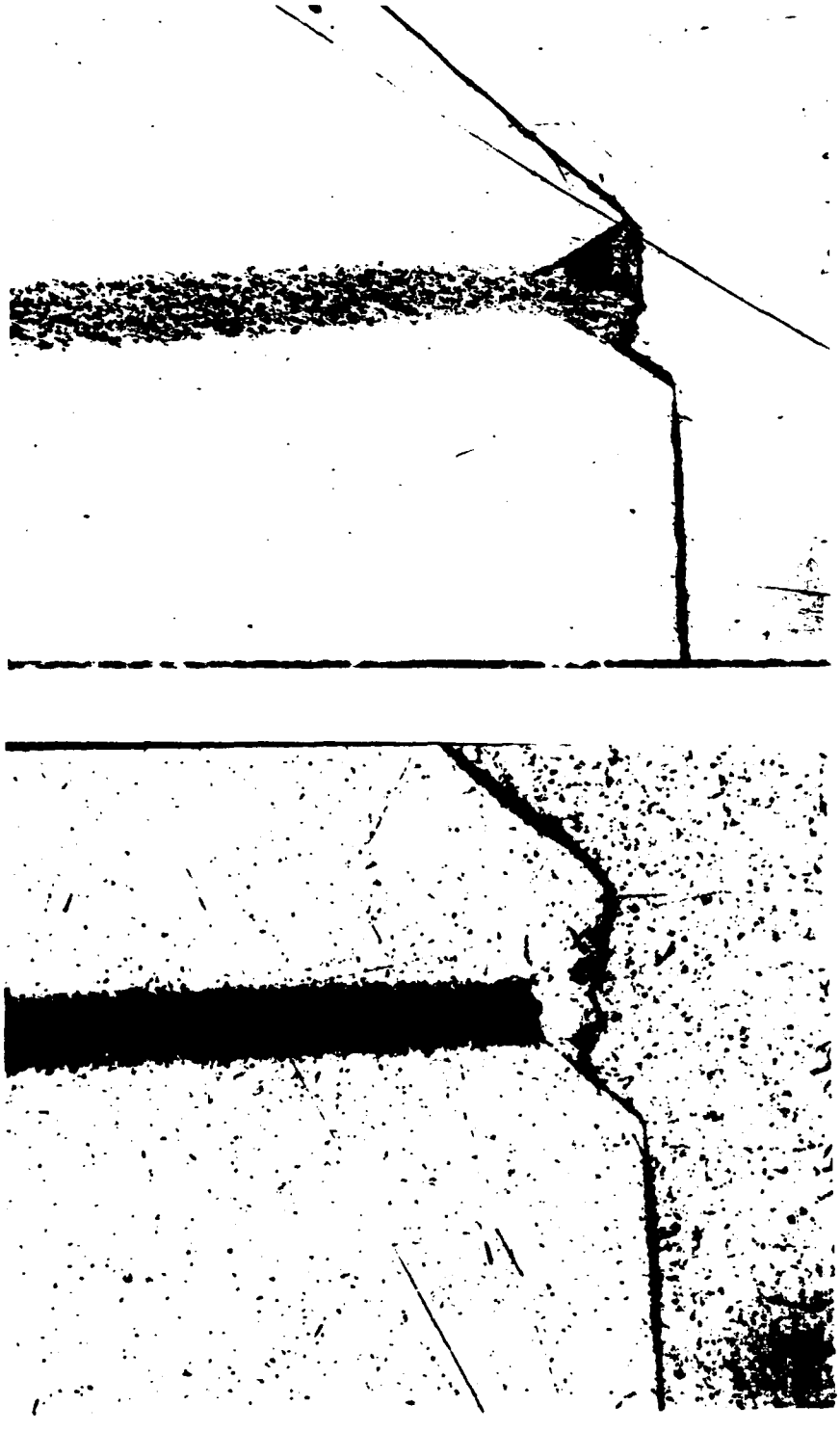

Figure 12: Comparison of Rivet Cross Sections from Two Panel Batches with Different Amounts of Rivet Deformation; Top - Batch 1; Bottom - Batch 2

Table 5: Comparison of Bucktail Diameter and Fatigue Lives for the Baseline Tests

Batch	Range of Average Bucktail Diameters (inches)	Average Cycles to First 0.1 inch Crack
1	0.235-0.237	48,700
2	0.250-0.251	96,400

Series I Testing: Study of the Terminating Action

The terminating action investigated in this study is the one described in SBR 737-53-1039 [2] for Boeing 737 aircraft with certain tail numbers. It is called a terminating action because its implementation "terminates" the need for more frequent maintenance checks. The steps of the action, in general terms, are:

a) Remove the flush head rivets from specified lap splice segments in the fuselage.

b) Drill out the rivet holes to accept a Universal (button head) rivet.

c) Inspect each rivet hole for cracks.

d) If no cracks are found, install the button head rivets. The terminating action is complete.

The technical basis for this action is apparently that enlarging the holes followed by inspection and using a different rivet geometry eliminates the knife edge stress concentration and any small cracks that may have initiated. (Note: the enlarged holes do not completely remove the taper.) The aircraft then resumes a normal and regular sequence of maintenance and inspection. The disadvantageous of the repair are primarily that it makes future inspection of rivet holes with sliding eddy current probes

more difficult and adds to aerodynamic drag.

The authors know of no prior published studies to validate the effectiveness of this terminating action repair.

Test Procedure

A series of 12-inch wide test panels was prepared for application of the terminating action by subjecting panels of the baseline configuration to various numbers of cycles. This prior damage ranged from zero cycles to enough cycles to create at least one crack that emanated 0.1 inches beyond the flush head rivet periphery. Unlike the actual, required terminating action, the rivet holes were not inspected for cracks after the holes were enlarged. The incorporation of cracked rivet holes in these tests was not meant to represent service - for such cracks should not escape detection - but to represent an extreme in prior damage. Panels were then fatigued after application of the terminating action for as many cycles as possible before failure occurred, which was always in a location other than the top row of rivets.

Table 6 lists the conditions and results of the terminating action tests conducted in pure tension. The results demonstrate a clear benefit of the terminating action to prevent the initiation and growth of cracks in the top row of rivets. Even when 0.1 inch long cracks were allowed to remain after the action, there was substantial retardation of crack growth. This is shown by a comparison of crack length increment vs. number of cycles for a flush head riveted panel and the terminating action panels for which some crack growth did occur, Figure 13.

Tests were discontinued, in all cases, when crack initiation and growth occurred from one of the very top row of rivets in the upper tear straps. Lap splice cracks were observed to initiate in the second (middle) row of rivets in the upper skin in two panels, but cracks were never observed to initiate in the lower row of rivets in the lower skin. This result is a bit surprising, since the lower row of holes in the lower skin experience higher

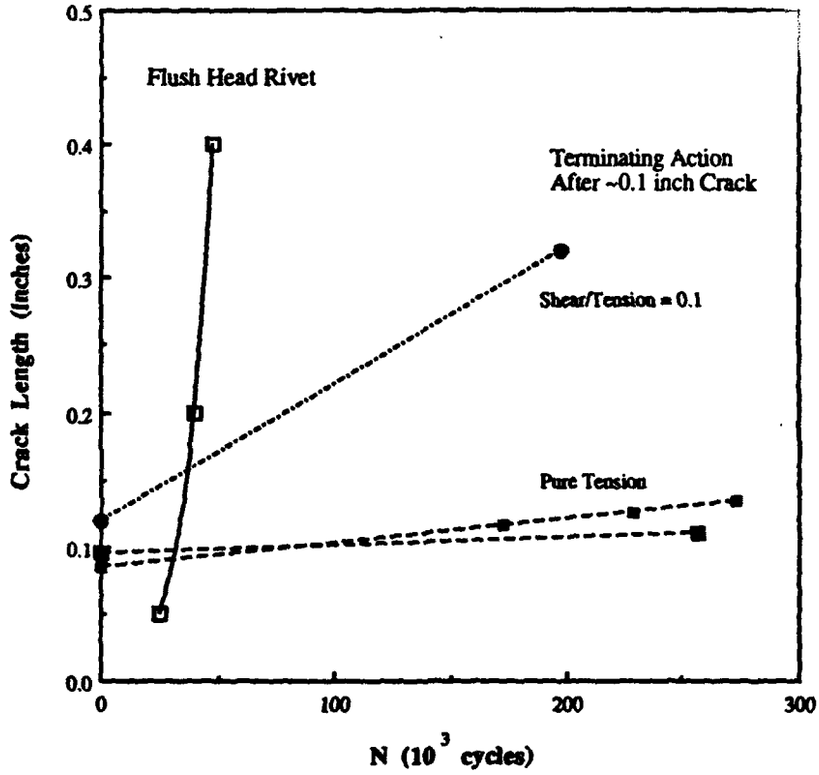

Figure 13: Comparison of Crack Growth Rates for a Baseline Test and for Terminating Action Tests

Table 6: Terminating Action Data
Maximum Nominal Stress = 16ksi (R=0.1); Tension Only

Specimen I.D.	Number of Cycles Prior to Termination Action	Max. Crack Length* prior to Terminating Action (inches)	Additional Cycles†	Incremental Crack Growth (inches)
12-B-4-1	0	0	338,280	0
12-B-4-2	0	0	254,270	0
12-B-4-3	0	0	290,370	0
12-FB-5B-1	45,000	0	350,000	0
12-FB-5B-2	45,000	0	304,180	0
12-FB-5A-1	77,650	0.020	129,480	0
12-FB-5A-2	66,900	0.020	328,360	0
12-FB-5D-1	127,260	0.097	257,080	0.012
12-FB-5D-2	72,890	0.084	294,000	0.063

*Crack length beyond flush rivet head periphery
†All tests in this series were discontinued because of cracking at the tear strap

membrane stresses than the second or middle row. Nevertheless, observation of second row cracking in a fuselage was reported in [1].

Some experiments were also conducted under combined shear and tension, in which the specimen maximum axial stress was maintained at 16ksi. The results, listed in Table 7, show that the terminating action is effective even with the addition of shear. Crack growth rate for those specimens containing 0.1 inch long cracks prior to the terminating action, also shown in Figure 13, is higher than in pure tension, perhaps due to the higher principal stress.

Thus, the results of this task provide strong evidence that fatigue life is greatly extended after application of the lap splice terminating action.

Series II Testing: The Effects of Superimposed Shear

A series of experiments was conducted to establish the effects of adding shear to tension on the fatigue life and formation of MSD for panels of the baseline configuration. As with the terminating action tests, the load magnitude was chosen to maintain a maximum stress of 16ksi along the long axis of the test panels. Initial tests with a shear-to-tension ratio of 0.2 often resulted in fatigue of the panel at the grips so that most tests were conducted at a ratio of 0.1. All specimens were taken from Batch 2 of the baseline configuration specimens.

Table 8 lists the results for the shear/tension tests and Figure 14 compares the results of all baseline tests. This figure shows the significant reduction in fatigue life caused by the addition of shear. Figure 15 shows a photograph of the cracks resulting from a test conducted at a shear-to-tension ratio of 0.2 and Figure 16 shows the crack pattern for one of the 0.1 ratio specimens in quantitative terms. Examination of Figure 16 and others like it - Appendix A - suggests that the addition of shear neither diminishes nor exacerbates the formation of MSD. However, there is a reduction in fatigue life which appears to be greater than expected from consideration of principal stress above. (This

Table 7: Shear/Tension Terminating Action Data; Maximum Axial Stress = 16ksi (R=0.1)

Specimen	Shear/Tension Ratio	Number of Cycles prior to Terminating Action	Max. Crack Length prior to Terminating Action (inches)	Additional Cycles*	Incremental Crack Growth (inches)
12-B-11-1	0.2	0	0	38,126	0
12-B-11-2	0.1	0	0	185,117	0
12-B-11-3	0.1	0	0	178,117	0
12-FB-12A-1	0.1	57,120	0.096	200,000	0
12-FB-12A-2	0.1	77,300	0.113	191,390	0.20
12-FB-12B-1	0.1	78,860	0.048	159,070	0

*Test terminated due to cracking away from lap splice.

Table 8: Fatigue Data for Combined Tension and Shear Loading;
Max. Nominal Stress = 16ksi; R=0.1
Baseline Configuration

Specimen	Shear/Tension Ratio	Cycles to First 0.1 inch Crack
12-F-10-1	0.2	28,800
12-F-10-2	0.2	>28,522*
12-F-10-3	0.1	61,000
12-FB-12A-1	0.1	57,120
12-FB-12A-2	0.1	74,538
12-FB-12B-1	0.1	>78,860*

* Test terminated due to cracking away from the lap splice

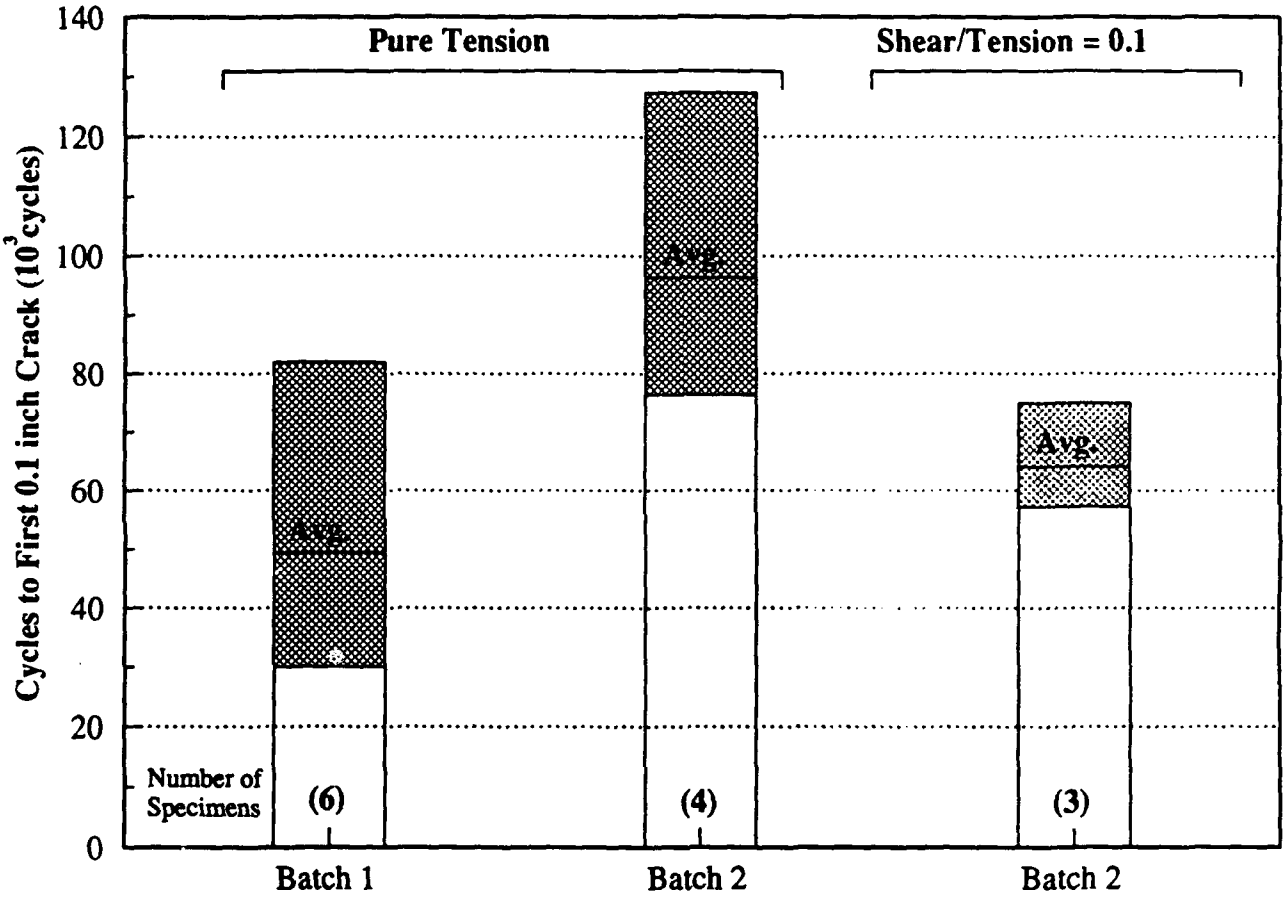

Figure 14: Results from all of the Baseline Tests

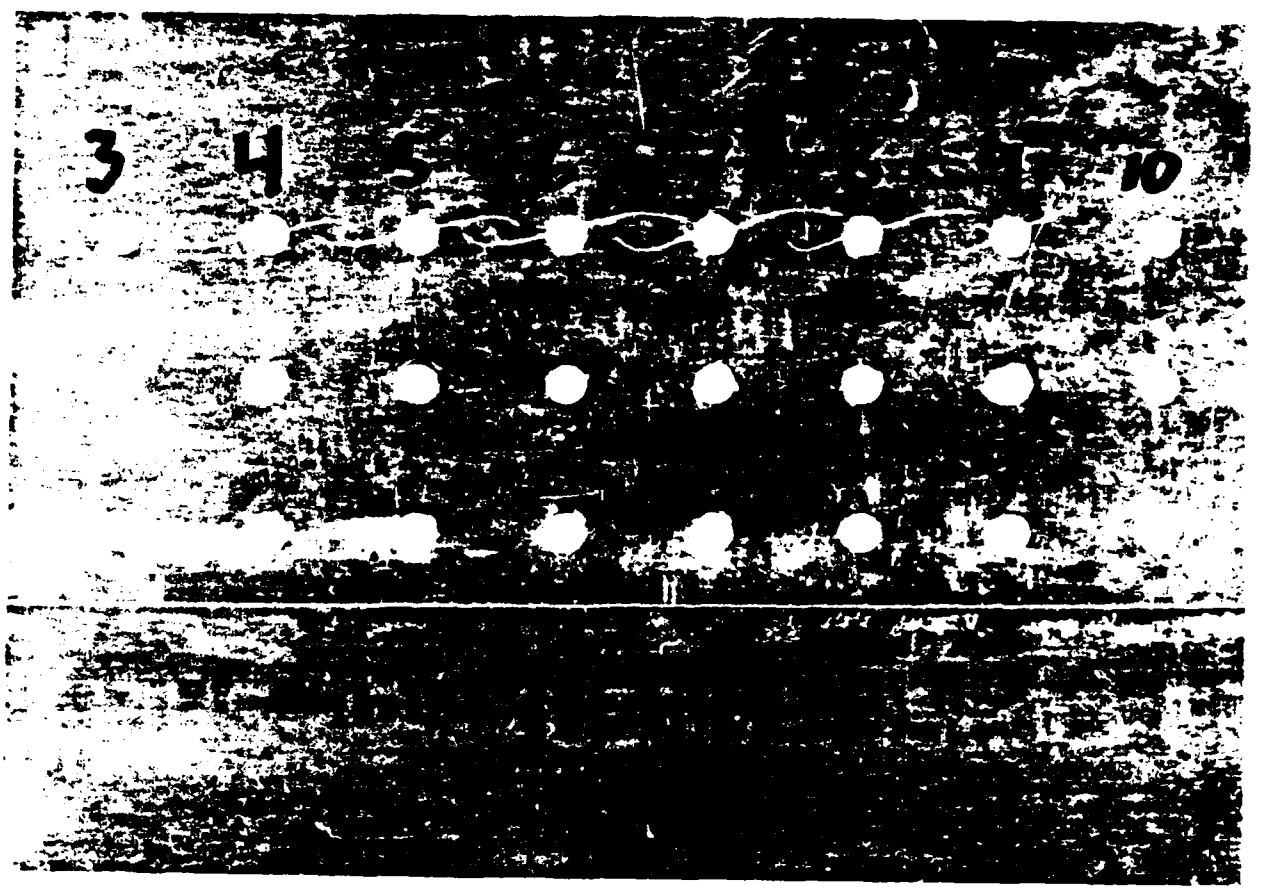

Figure 15: An Example of the Cracking Pattern for a Panel Tested at a Shear-to-Tension Ratio of 0.2

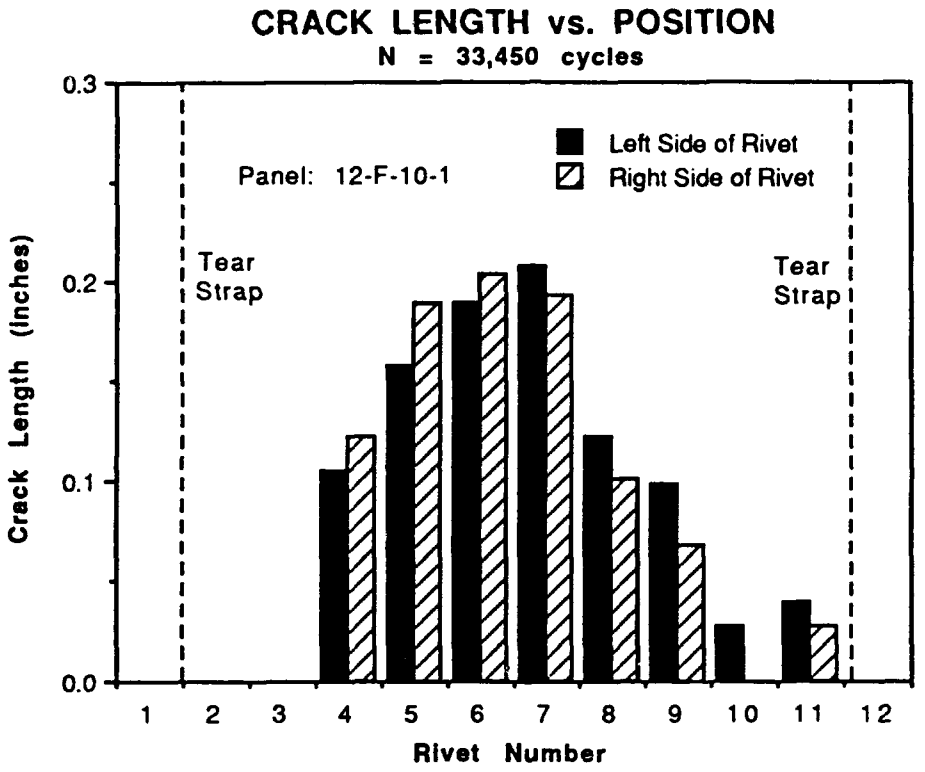

Figure 16: The Crack Pattern from one of the Shear/Tension Tests

point is treated further in the Discussion section.)

Series III Testing: Study of the Effects of Lap Splice Parameters on Fatigue

The Aloha Airlines accident was attributed in part to a fuselage lap splice design that was peculiar to a certain type of aircraft. In addition to the loss of bonding, use of very thin skin - 0.036 inches - for weight reduction resulted in the formation of a knife edge stress riser that caused earlier than expected fatigue. A natural question is whether such early fatigue and MSD formation can occur in other lap splice configurations with different models and newer aircraft. It is also interesting to determine whether variations within a particular type of lap splice design due, say, to manufacturing variability, can have an effect on MSD.

This test series was divided into two parts: A and B. In Series IIIA a relatively large array of panel configurations was studied to identify dominant effects. More detailed tests with only a few parameters were tested in the second part.

Series IIIA

The parameters and their levels selected for testing in Series IIIA are listed in Table 9. The rationale for their inclusion in this test program is the following: Stress level is one of the principal variables between aircraft designs. It is our understanding that the nominal hoop stress in parts of the 727 fuselage is 13ksi while some lap splices in the 747 can experience nominal stress values as high as 18ksi. The Briles rivet type, a cross section of which is shown in Figure 17, was tested because this rivet has been used in the B767 and is apparently under consideration for other aircraft. Its advantage may arise from the elimination of the knife edge-type stress riser by use of a 120° head with a top cylindrical portion. Our examination of aircraft lap splices shows that several values of rivet spacing are used in construction. The values of 0.75 and 1.29 inches are convenient values that result in uniform rivet spacing across the 12-inch width of the specimen between the tear straps. The inclusion of a continuous and staggered rivet orientation is

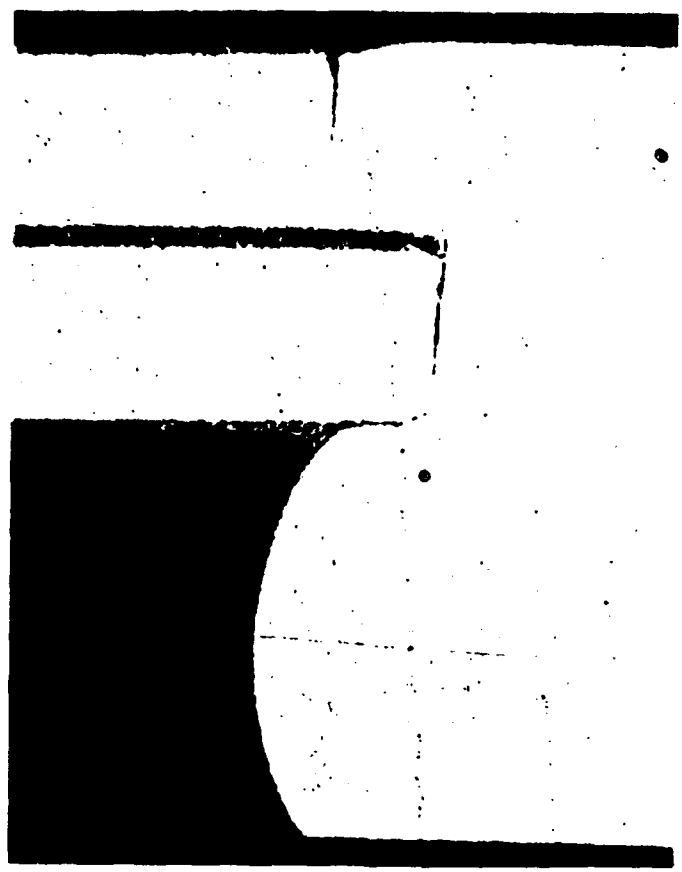

Figure 17: Cross Section of a Briles Rivet in 0.040 inch Thick Sheets

based on the observation that rivets do not always line up in a row. Figure 18 shows the geometry of the staggered orientation tested, with a photograph of a piece from an actual lap splice. A number of rows equal to five was selected to represent more than three rows while maintaining symmetry with respect to the piece of metal representing the stringer. Finally, three sheet or skin thicknesses were selected to cover the range that can be found on commercial aircraft.

Table 9: Parameters Investigated in the Statistically Designed Test Matrix

Parameter	Levels Tested
Stress level:	12, 14 and 16ksi
Rivet type:	flush head and Briles
Rivet spacing:	0.75, 1.00 and 1.29 inches
Rivet orientation:	continuous and staggered
Number of rivet rows:	3 and 5
Skin thickness:	0.040, 0.050 and 0.063 inches

Experimental Design Considerations

Examination of Table 9 indicates that three of the parameters of interest occur at three test levels, and three others at two levels. Consequently, a total of 216 ($3^3 \times 2^3$) unique panel configurations could have been constructed for this test series. However, by utilizing the principles of statistical experimental design, a fractional factorial plan was selected to ensure that all important effects of these six parameters could be evaluated, while simultaneously ensuring that the experiment was efficient in terms of size and cost.

As stated in [8,9] fractional factorial experiments are commonly used in multifactor experiments for the following reasons:

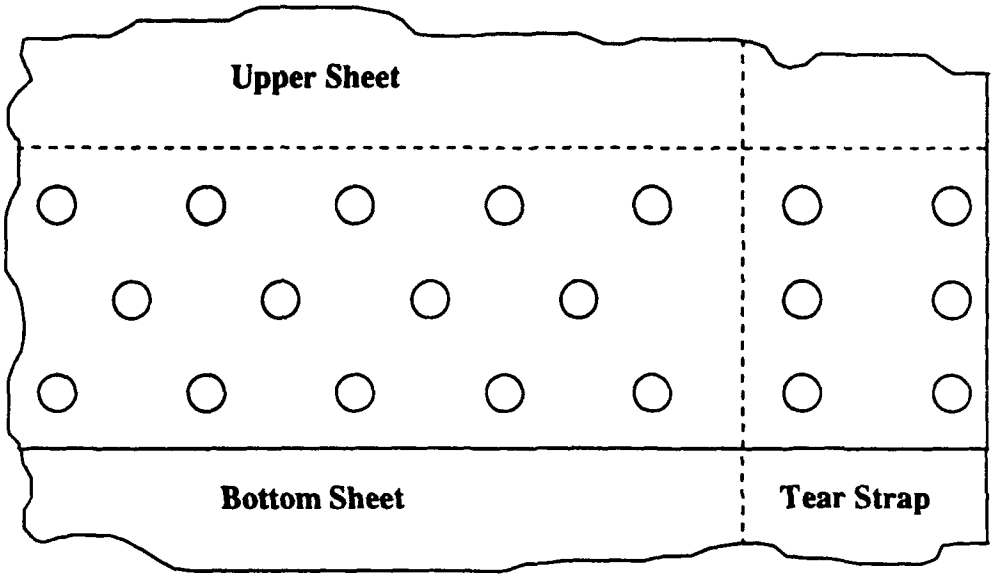

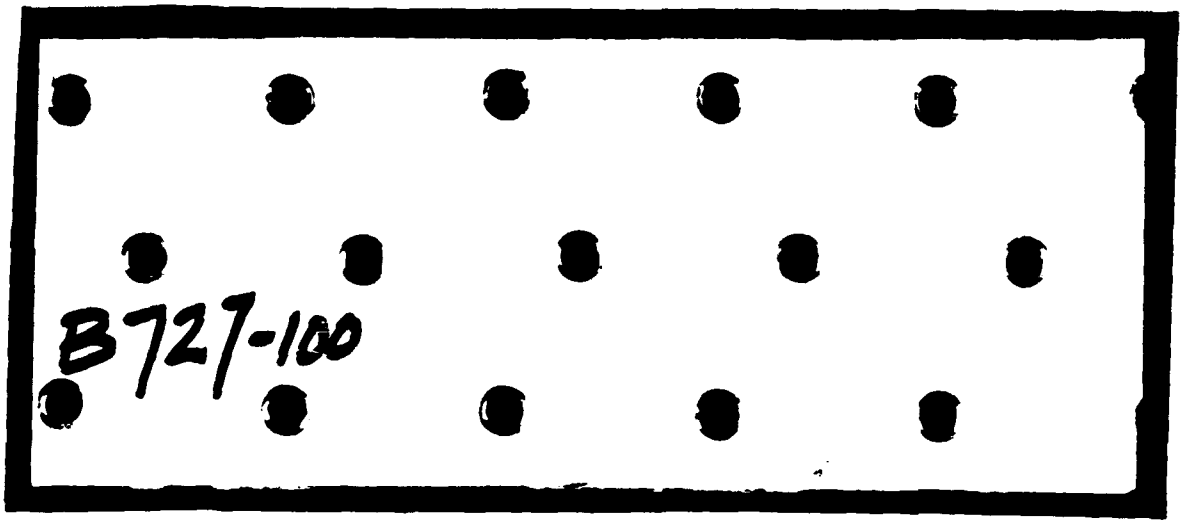

Figure 18: The Geometry of the Staggered Rivet Orientation Tested (top) Compared to a Sample from a B727 Fuselage (bottom)

(i) the joint effects of two (or more) parameters on a response (e.g., crack initiation) can be investigated only by simultaneously changing two or more of the parameters; joint effects are called "interactions" in the statistical literature;

(ii) great economies of time and experimental resources are achieved because each test run provides information on all factors considered in the experiment; and

(iii) the conclusions and inferences are generally applicable to a wide range of configurations, since several factors have been changed overall; this wide applicability would not occur from an experiment in which one or very few factors are changed while others are held fixed.

Although many options were available, it was decided to use a fractional factorial plan consisting of 27 unique test configurations. The rational for determining an adequate number of test runs is quite complex, since it requires a thorough understanding of the following key aspects of the total experimental program:

(i) most importantly, the overall objective of the experiment itself, including how the results and conclusions will be acted upon;

(ii) specific engineering and/or scientific requirements to be considered in designing, conducting, analyzing, and interpreting the outcome of the experiment;

(iii) available resources (budgetary, time, equipment, personnel, etc.); and

(iv) statistical and data-analytic issues, including:

- specification of effects and/or parameters to be estimated (both individual and joint, or "interactive," effects);

- determining the relevant magnitude of an effect; that is, how large should it be in order to be considered to have an "appreciable" impact on the response being measured;

- recognition of risk levels to be tolerated; that is, what are the consequences of falsely concluding that a factor does or does not have a dominant effect; these risks are referred to as Type I and Type II errors in the statistical literature; and

- the expected reproducibility of test measurements; that is, the inherent variation anticipated between results obtained from running identical test conditions; this source of variation is called the experimental error.

All of these elements contributed to the collaborative decision to use the fractional factorial plan depicted in Table 10. A key consideration in the selection of this particular plan was that it yields unbiased (and uncorrelated) estimates of the effect uniquely attributable to varying the levels of each of the six parameters independently. Such effects are commonly called "Main Effects" and are defined as the change that occurs in the average value (of cycles-to-failure or MSD in the experiment) corresponding to the change in the levels specifically considered in the test. Such effects can be formally tested, using the concept of a statistical "significance test", which is one way of assessing the relative importance of varying each factor over its corresponding levels.

With the design given in Table 10, it was also possible to estimate certain pre-determined joint effects, or interactions. Specifically, the interaction of stress with skin thickness, stress with rivet spacing, and skin thickness with rivet spacing could also be evaluated using this test plan.

Table 10: The 27 Combinations of Parameters Tested in Series IIIA

Number	Stress (ksi)	Rivet Type	Rivet Spacing (inch)	Rivet Orientation	No. of Rows	Thickness (inch)
1	12	Flush	1.00	Staggered	5	0.040
2	12	Briles	1.00	Staggered	3	0.050
3	12	Flush	1.00	Continuous	5	0.063
4	12	Briles	1.29	Continuous	5	0.040
5	12	Flush	1.29	Staggered	5	0.050
6	12	Flush	1.29	Staggered	3	0.063
7	12	Flush	0.75	Staggered	3	0.040
8	12	Flush	0.75	Continuous	5	0.050
9	12	Briles	0.75	Staggered	5	0.063
10	14	Briles	1.00	Continuous	3	0.040
11	14	Flush	1.00	Staggered	5	0.050
12	14	Flush	1.00	Staggered	5	0.063
13	14	Flush	1.29	Staggered	5	0.040
14	14	Flush	1.29	Continuous	3	0.050
15	14	Briles	1.29	Staggered	5	0.063
16	14	Flush	0.75	Staggered	5	0.040
17	14	Briles	0.75	Staggered	5	0.050
18	14	Flush	0.75	Continuous	3	0.063
19	16	Flush	1.00	Staggered	5	0.040
20	16	Flush	1.00	Continuous	5	0.050
21	16	Briles	1.00	Staggered	3	0.063
22	16	Flush	1.29	Staggered	3	0.040
23	16	Briles	1.29	Staggered	5	0.050
24	16	Flush	1.29	Continuous	5	0.063
25	16	Briles	0.75	Continuous	5	0.040
26	16	Flush	0.75	Staggered	3	0.050
27	16	Flush	0.75	Staggered	5	0.063

All tests were conducted according to the baseline procedures described previously. Repeat tests were performed on many of the 27 configurations in order to reduce the effect of inherent variability when looking for dominant effects attributable to the six factors and three interactions. Stated another way, these repeat tests enabled us to generate a more precise estimate of experimental error, which is a critical component in carrying out the analysis. All of the test results are given in Appendix C.

Measurements (Definition of Response Variables)

Quantitative definitions were required for both fatigue life and MSD to perform the statistical analysis described below. As before, fatigue life was defined as the number of cycles required to grow the first crack to 0.1 inch in the top row of rivets. MSD was more difficult to define. To our knowledge, no measures have been generally accepted to date. Derivation of the measure used in this study is given in Appendix D. It is a restatement of the net section yield criterion of fracture for uniform MSD:

$$MSD=\left(\frac{W'}{\Sigma l_i}-1\right)/\left(\frac{\sigma_f}{\sigma_n}\frac{W'}{W}-1\right);\ \textit{evaluated at}\ a_{max}=0.25\ \textit{inch} \qquad (1)$$

where W = width of the specimen

$W' = W - nd_{rivet}$

n = number of rivets in the top row

d_{rivet} = diameter of the rivet head

Σl_i = sum of the remaining ligament lengths at a_{max} = 0.25 inches

a_{max} = longest crack length from rivet head

σ_f = flow strength of the aluminum (average of yield and tensile strengths - 48,500 lb/in^2)

σ_n = nominal stress applied in the test,

with the following properties:

MSD = 1 for predicted fracture (strictly only for uniform MSD) and

MSD = 0 for no cracks.

As an example, suppose that 50% of the rivet holes in a baseline panel had a crack equal to 0.25 inches emanating from each side and the remaining rivet holes had no cracks. Then MSD = 0.28.

The original intent in this task was to test duplicate specimens for each of the 27 unique combinations given in Table 10. It was subsequently decided to perform some of the tests intended for a stress level of 12ksi at 18ksi and, in fact, three tests were performed inadvertently at 27ksi. However, only the 12-16ksi results were included in the statistical analysis discussed in the next section. In those cases for which duplicate specimens were tested, the fatigue lives were averaged prior to data analysis in order to retain the factor/level balance mentioned earlier.

Not all panels were tested to failure. In some tests, cracking only occurred at the reinforcing tear straps - an artificial detail - or the test was terminated when a large number of cycles were accumulated, usually at approximately 400,000. Panels that did not fail during the test are called censored panels. An estimation procedure was used to account for fatigue life of such panels; that is, for panels that did not fail during the test. A graphical analysis at each stress level indicated that the cycles-to-failure data could be characterized by a Weibull probability function; namely,

$$F(N) = 1 - \exp[-(N/N_o)^m],$$

where

$F(N)$ = probability of failure prior to N cycles

N_o = characteristic life (the scale parameter)

m = Weibull modulus (the shape parameter).

The parameters N_o and m were estimated separately from graphs plotted for each of the three stress levels considered. In all three cases the fit of the data to the Weibull distribution was reasonably close; Figure 19 illustrates the goodness-of-fit for results obtained at 14ksi. Although only those panels that actually failed appear on the plot, all test panels were used in determining the failure rate that is depicted in Figure 19. This probability equation was then used to estimate the expected life of unfailed specimens based on the number of cycles they had survived according to computational procedures described in [10]. No censored data were analyzed for MSD.

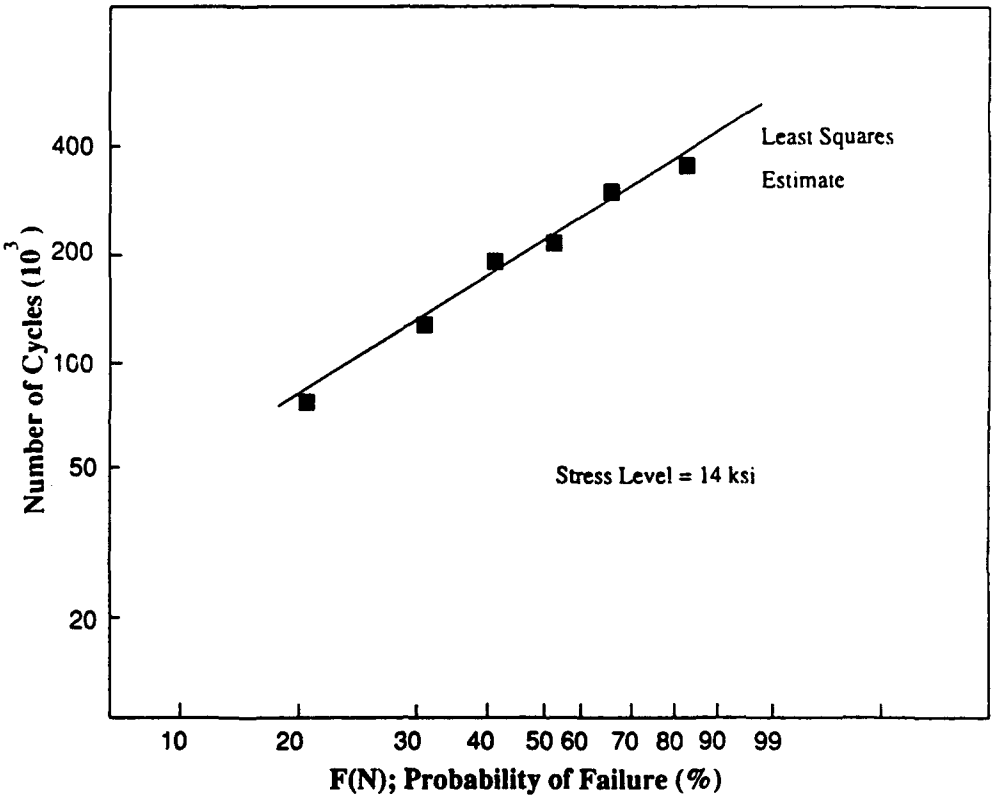

Figure 19: An Example of the Fit of Data From Series IIIA to a Weibull Curve

Statistical Analysis of Fatigue Life Data

Statistical inference procedures for analyzing data from a fractional factorial experiment often include the use of the Analysis of Variance (ANOVA) partitioning method. With this method, the variation observed in the fatigue life data is sub-divided into two major components; namely,

(i) variation due to assignable causes; i.e., the effects uniquely attributable to the factors controlled in designing and running the test; and

(ii) variation due to random or uncontrolled sources, which account for the inherent (and inescapable) fact that identical panels will not yield the same cycles-to-failure measurements in repeated testing.

For convenience, the fatigue life measurements given in Appendix C are summarized in Figure 20. In this table duplicate test panel measurements have been averaged; furthermore, failure times have been estimated for those panels that were not tested to failure.

Fatigue life measurements ranged from 63,000 cycles (for Test Panel #20) to 1,333,000 cycles (for Test Panel #9 which did not actually fail during testing). The fundamental questions are (i) why do measurements vary over these 27 tests panels? And more importantly, (ii) can this variability be attributable to specific parameters that were controlled from the outset?

The underlying theory and computational aspects of ANOVA are rather complex, but are thoroughly documented in most statistical methods texts; excellent discussions appear in [9, 11]. Essentially, the technique is based on the fact that up to 26 quantities (i.e., independent estimates) can be derived from the 27 data points; that is, there are 26 degrees of freedom with which to work. As an example, one degree of freedom could be used to construct an estimate of the difference between the cycles-to-failure observed for

Aging Aircraft Study
Original Data

OBS	TESTNUM	STRESS	RIVTYPE	RIVSPACE	RORIENT	NUMROWS	SKINTHK	TESTLOC	_TYPE_	_FREQ_	CYCLES	MSD	LCYCLES
1	1	12	Flush	1.00	Staggered	5	0.040	FTI	0	1	873600	.	5.94131
2	2	12	Briles	1.00	Staggered	3	0.050	FTI	0	1	1210000	.	6.08279
3	3	12	Flush	1.00	Cont.	5	0.063	ADL	0	1	526700	0.021	5.72156
4	4	12	Briles	1.29	Cont.	5	0.040	FTI	0	1	1097000	.	6.04021
5	5	12	Flush	1.29	Staggered	5	0.050	ADL	0	1	175766	0.016	5.24493
6	6	12	Flush	1.29	Staggered	3	0.063	FTI	0	1	175000	0.020	5.24304
7	7	12	Flush	0.75	Staggered	3	0.040	ADL	0	1	662000	.	5.82088
8	8	12	Flush	0.75	Cont.	5	0.050	FTI	0	1	350000	0.022	5.54407
9	9	12	Briles	0.75	Staggered	5	0.063	FTI	0	1	1333000	.	6.12483
10	10	14	Briles	1.00	Cont.	3	0.040	ADL	0	1	510500	.	5.70800
11	11	14	Flush	1.00	Staggered	5	0.050	FTI	0	2	134000	0.038	5.12710
12	12	14	Flush	1.00	Staggered	5	0.063	FTI	0	2	226000	0.030	5.35411
13	13	14	Flush	1.29	Staggered	5	0.040	FTI	0	2	388000	0.022	5.58585
14	14	14	Flush	1.29	Cont.	3	0.050	FTI	0	2	81500	0.023	4.91118
15	15	14	Briles	1.29	Staggered	5	0.063	ADL	0	2	468910	.	5.67109
16	16	14	Flush	0.75	Staggered	5	0.040	FTI	0	2	524950	.	5.72012
17	17	14	Briles	0.75	Staggered	5	0.050	ADL	0	2	540100	.	5.73247
18	18	14	Flush	0.75	Cont.	3	0.063	FTI	0	2	194000	0.049	5.28780
19	19	16	Flush	1.00	Staggered	5	0.040	FTI	0	2	311000	0.044	5.49276
20	20	16	Flush	1.00	Cont.	5	0.050	ADL	0	2	83000	0.031	4.79934
21	21	16	Briles	1.00	Staggered	3	0.063	FTI	0	2	117500	0.049	5.07004
22	22	16	Flush	1.29	Staggered	3	0.040	ADL	0	2	133000	0.033	5.12385
23	23	16	Briles	1.29	Staggered	5	0.050	FTI	0	2	289000	.	5.46090
24	24	16	Flush	1.29	Cont.	5	0.063	FTI	0	2	71500	0.046	4.85431
25	25	16	Briles	0.75	Cont.	5	0.040	FTI	0	2	303800	.	5.48259
26	26	16	Flush	0.75	Staggered	3	0.050	FTI	0	2	80000	0.064	4.90309
27	27	16	Flush	0.75	Staggered	5	0.063	ADL	0	2	251323	0.039	5.40023

Figure 20: Summary of the Series IIIA Data Used in the Statistical Analysis

flush head rivets as opposed to Briles rivets. For this comparison, the results are shown in Table 11.

Table 11: An Example of the Effect of One Parameter

		Cycles-to-Failure	
Rivet Type	**No. of Panels Tested**	**(Average)**	**(Median)**
Flush	18	289,000	210,000
Briles	9	652,000	510,000

The average values are substantially larger than the corresponding medians due to the influence of a few very large failure times. Even though this observed difference of at least 300,000 cycles (which is uniquely attributable to rivet type) is numerically large, it is still necessary to compare it to some measure of inherent variability before concluding that it is indeed "real," appreciable, and reproducible.

The ANOVA technique performs such a task. However, a few of the computational aspects of the method should be clarified at this point. First, instead of using simple averages or medians as illustrated above, comparisons are made using "Sums of Squared" observations. The concept is the same; namely, degrees of freedom are used to construct estimates of well-defined quantities that are uniquely attributable to each of the parameters controlled in the experiment. Second, as with the application of any analytical method, certain assumptions are required. One important assumption is that the aforementioned uncontrolled source of variation follows a normal probability distribution. To satisfy this critical assumption, it was necessary to transform the data and analyze the logarithm of cycles-to-failure for this experiment.

Finally, statistical inferences concerning effects and interactions using ANOVA are based on F-statistics, which are ratios of Mean Squares. Mean Squares are calculated by dividing the Sum of Squares by the corresponding degrees of freedom. A large F-statistic indicates that the corresponding parameter has an effect on cycles-to-failure that greatly

exceeds the effect of normal variation inherent in the data.

Equivalent to the F-statistic is a corresponding p-value. A p-value (or significance probability) is the theoretical probability of obtaining an F-value as large or larger than the one actually observed in the experiment if, in fact, the parameter has no effect whatsoever on cycles-to-failure. Consequently, a small p-value, usually taken as 0.10 or less, indicates a "significant" or dominant effect due to varying the factor over different levels.

The ANOVA table for fatigue life data (log cycles to failure) is summarized in Table 12 below; the complete output generated by the commercially available SAS[12] software package is given in Appendix C.

Table 12: ANOVA Table -- Fatigue Life (log cycles-to-failure)

Source of Variation	Degrees of Freedom	Sum of Squares	Mean Square	F-Value*	p-Value
Stress	2	1.489	0.74	16.5	0.01
Rivet Type	1	0.829	0.83	18.4	0.01
Spacing	2	0.205	0.10	2.3	0.22
Orientation	1	0.105	0.10	2.3	0.20
No. Rows	1	0.164	0.16	3.6	0.13
Skin Thickness	2	0.559	0.28	6.2	0.06
Test Lab (Dummy)	1	0.001	0.001	0.02	0.89
Stress x Spacing	4	0.177	0.04	1.0	0.51
Stress x Thickness	4	0.016	0.004	0.1	0.98
Spacing x Thickness	4	0.067	0.02	0.4	0.82
Exper. Error	4	0.180	0.045	--	
Total	26	3.793			

* F-Value = (Mean Square for Effect)/(Exper. Error Mean Square)

Inspection of the p-values in the ANOVA, (Table 12) reveals that three of the factors tested had a dominant influence on fatigue life for the 12-inch wide, reinforced panel. Varying the stress level, rivet type, and skin thickness had an appreciable impact on cycles-to-failure. The interpretation of significance testing as reflected by the p-value can be illustrated by considering the aforementioned rivet type data. As noted, the test panels with Briles rivets yielded more than a two-fold increase in fatigue life when compared to the flush head rivets. This observed difference can now be related to inherent variability expected in the fatigue life of test panels by examining the experimental error entry in the ANOVA table. Since the Mean Square Error term (0.045) measures inherent variance in the data, its square root corresponds to a standard deviation; $\sqrt{0.045} = 0.21$ for these data.

Since we are analyzing the logarithm of cycles-to-failure, an observed difference in logarithms is equivalent to the ratio of the two quantities being compared. Therefore, a difference between logarithms of 0.21 (i.e., one standard deviation in random error) is equivalent to about a 62% difference in a ratio ($10^{0.21} = 1.62$). Considering the ratio of cycles-to-failure for Briles rivets/flush head rivets, it is now evident that this ratio (expressed as a ratio of either means or medians) far exceeds the 1.62 value characterizing random variability.

Finally, a few more conditions must be recognized as well; namely,

(i) we are comparing means; in fact, we are actually comparing estimates of means;

(ii) an estimate based on nine observations is less precise than an estimate based on 18 observations; that is, the precision depends on the number of observations or, equivalently, the degrees of freedom;

(iii) a variation of only one standard deviation is generally not regarded as "large" or unusual; in fact, by definition, it's expected to be exceeded about 32% of the time;

(iv) however, differences exceeding two standard deviations are unlikely since they should occur only about 5% of the time.

All of these considerations enter into a rigorous significance test procedure. Fortunately, the computational process is streamlined, and the key results are given below in Figure 21:

```
                    Aging Aircraft Study
                    Full Model - 27 obs - Bal

                  General Linear Models Procedure

               T tests (LSD) for variable: LCYCLES

NOTE: This test controls the type I comparisonwise error rate

                Alpha= 0.05  df= 4  MSE= 0.045088
                    Critical Value of T= 2.78
                Least Significant Difference= 0.2407
                WARNING: Cell sizes are not equal.
                 Harmonic Mean of cell sizes= 12

Means with the same letter are not significantly different.

      T Grouping          Mean      N  RIVTYPE

               A        5.7081      9  Briles

               B        5.3364     18  Flush
```

Figure 21: An Example of the Output from SAS for Rivet Type

The two means (of log cycles) are seen to be significantly different, since their difference of 0.37 far exceeds the Least Significant Difference (0.24), which serves as a test criterion based on the four conditions stated above. Note that the difference of 0.24 in logarithms translates to a ratio of $10^{0.24} = 1.74$. Therefore, we would have concluded in this experiment that Briles rivets lead to a significantly longer fatigue life in test panels, as long as the Briles cycles-to-failure were at least 1.74 times greater than flush head lives. In other words, this experiment ultimately was capable of detecting a difference of this magnitude (which, of course, could only have been surmised at the very outset of the program).

Based on the ANOVA table the three significant factors appear to be acting independently, since none of the three estimable interactive effects were dramatically different from the error term. Although there is some evidence that rivet spacing, orientation, and the number of rows have an impact on cycles to failure, the effect is clearly of lesser magnitude than the other three factors, and is only marginally greater than variability attributable to experimental error itself. Further tests would be required to confirm that these apparently numerically smaller effects are indeed real and reproducible.

Table 13 summarizes the fatigue life test results. For convenience, median values of cycles-to-failure are tabulated; as indicated above, the levels within each parameter tested are declared significantly different from one another on the basis of analyzing logarithms of the individual observations using the ANOVA technique.

These data show that the effect of stress level and rivet type on fatigue life are as expected; lower stress levels increase fatigue life and the Briles rivet, which eliminates the knife edge, also increases fatigue life. On the other hand, the effect of skin thickness is counter intuitive; the greatest life is obtained with the smallest skin thickness, even though the knife edge is sharpest in this configuration. This is an important point because the use of thicker skins in aircraft is being partially relied upon to prevent the occurrence of early fatigue. Additional tests, described in the next section, were performed in Series IIIB to examine this effect more closely.

Statistical Analysis of MSD Data

The analysis of MSD results was limited to specimens fabricated with standard, flush head rivets because only one of the nine Briles rivet configurations developed cracks. Even a complete set of the flush head rivet data was not available because fatigue did not always initiate in the lap splice area in some of the specimens before termination of the test. Unlike the analysis for fatigue life, there was no obvious method to utilize these censored observations. Nevertheless, the ANOVA methodology is designed to

compensate for incomplete data sets.

The results of the analysis, shown in Figure 22 and summarized in Table 14, indicate that only the stress parameter appears to have a significant effect on MSD. (Appendix C includes the individual MSD data and the output form SAS.) .

Table 13: Summary of Series IIIA Test Results: Fatigue Life

Parameter	Level	No. of Test Panels	Median Fatigue Life (Cycles)	ANOVA Outcome
Stress	12 ksi 14 ksi 16 ksi	9 9 9	662,000 368,000 117,500	All three levels are significantly different
Rivet type	Flush Briles	18 9	219,000 510,000	Levels are significantly different
Rivet spacing	0.75 in 1.00 in 1.29 in	9 9 9	350,600 311,900 175,800	No statistical difference
Rivet orientation	Continuous Staggered	9 18	303,000 300,400	No statistical difference
No. of rows	3 rows 5 rows	9 18	175,000 326,900	No statistical difference
Thickness	0.040 in 0.050 in 0.063 in	9 9 9	510,500 175,800 226,000	Thickness of 0.04 in yielded significantly longer life

Aging Aircraft Study
Flush Only

General Linear Models Procedure

Dependent Variable: MSD

Source	DF	Sum of Squares	Mean Square	F Value	Pr > F
Model	8	0.00192660	0.00024083	2.42	0.1491
Error	6	0.00059780	0.00009963		
Corrected Total	14	0.00252440			

R-Square	C.V.	Root MSE	MSD Mean
0.763193	30.06512	0.00998162	0.03320000

Source	DF	Type IV SS	Mean Square	F Value	Pr > F
STRESS	2	0.00094530	0.00047265	4.74	0.0581
RIVSPACE	2	0.00034293	0.00017147	1.72	0.2568
RORIENT	1	0.00001875	0.00001875	0.19	0.6796
NUMROWS	1	0.00009754	0.00009754	0.98	0.3607
SKINTHK	2	0.00004101	0.00002051	0.21	0.8195

Figure 22: Summary of Statistical Analysis of Series IIIA MSD Data

Table 14: Summary of Series IIIA Statistical Analysis Results: MSD (Flush head rivets only)

Parameter	Level	No. of Test Panels	Average MSD	ANOVA Outcome
Stress	12 ksi 14 ksi 16 ksi	4 5 6	0.020 0.032 0.043	Evidence of a difference in MSD between 12 and 16 ksi
Rivet spacing	0.75 in 1.00 in 1.29 in	4 5 6	0.044 0.033 0.027	No statistical difference
Rivet orientation	Continuous Staggered	6 9	0.032 0.034	No statistical difference
No. of rows	3 rows 5 rows	5 10	0.038 0.031	No statistical difference
Thickness	0.040 in 0.050 in 0.063 in	3 6 6	0.033 0.032 0.034	No statistical difference

The monotonic increase in MSD with stress level suggests that additional tests may show a highly significant effect of this variable. No significant effect of thickness on MSD was observed or indicated.

Average MSD values are relatively low, corresponding to the equivalent of only two or three cracks of equal 0.25 inch size (Appendix D). The largest value of MSD in the stress range of 12-16ksi was 0.088, or the equivalent of five cracks of equal size. Nevertheless, some of the specimens had as many as 8-10 individual rivet hole cracks at the completion of testing. Figure 23 shows the distribution of top row rivet hole edge cracks at the completion of testing for all specimens tested in Series IIIA.

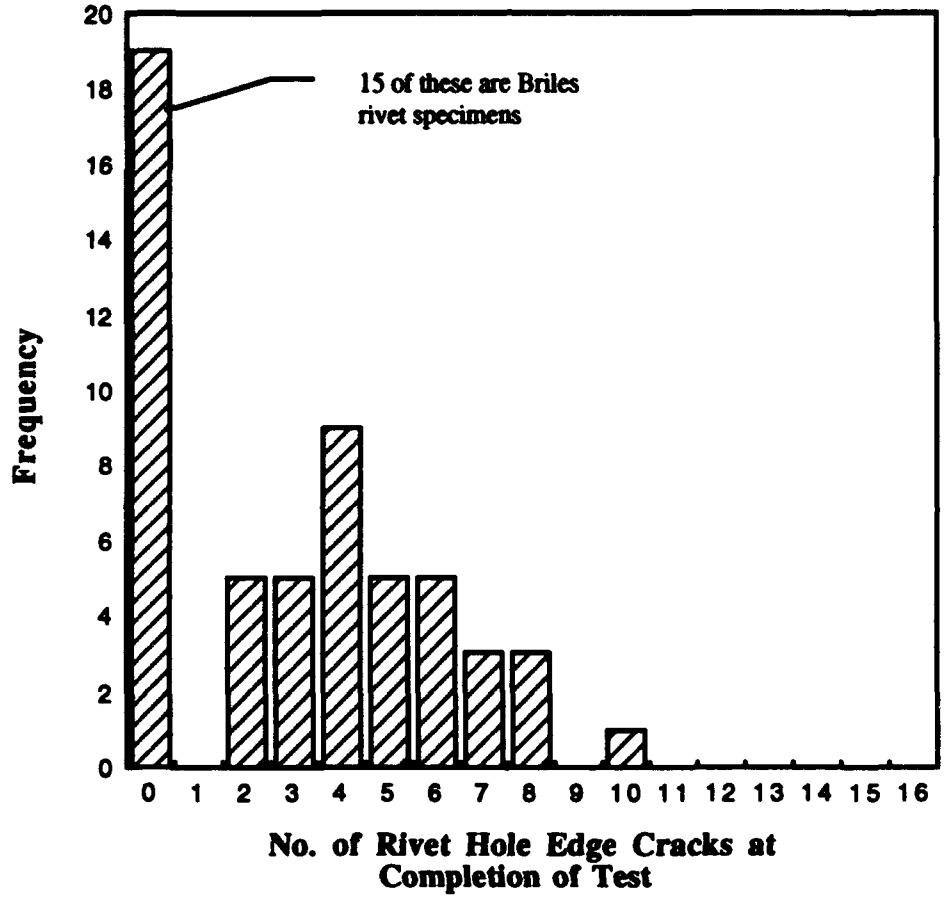

Figure 23: The Distribution of Number of Cracks in Series IIIA Panels

Series IIIB

The results of Series IIIA pointed to the need for additional testing of two important parameters: skin thickness and stress level. Table 15 lists the test variables for this next series; all other parameters followed the baseline configuration. Both stress and thickness ranges were expanded to test at levels exceeding those considered in Series IIIA in an effort to determine whether the MSD effect would be observed over a broader range of test conditions.

Table 15: Series IIIB Test Parameters

Number of Tests			
	Thickness		
Stress	0.040 in	0.063 in	0.080 in
14 ksi	5	-	-
18 ksi	5	3	4
20 ksi	4	-	-

A summary of the results is listed in Table 16 for fatigue life and Table 17 for MSD; detailed results are included in Appendix C.

Table 16: Summary of Series IIIB Test Results - Fatigue Life

Parameter	Level	No. of Test Panels	Median Fatigue Life (cycles)	ANOVA Outcome
Stress[a]	14 ksi 18 ksi 20 ksi	5 5 4	109,200 48,300 29,200	All three levels are significantly different
Thickness[b]	0.040 in 0.063 in 0.080 in	5 3 4	48,300 61,800 72,500	Fatigue life for 0.040 inch is significantly less than for 0.063 and 0.080 inch

(a) At 0.040 in thickness only
(b) At 18 ksi stress level only

Table 17: Summary of Series IIIB Test Results: MSD

Parameter	Level	No. of Test Panels	Average MSD	ANOVA Outcome
Stress[a]	14 ksi 18 ksi 20 ksi	5 5 4	0.043 0.107 0.150	14 ksi stress yielded significantly lower MSD than other stress levels
Thickness[b]	0.040 in 0.063 in 0.080 in	5 3 4	0.107 0.147 0.050	All three levels are significantly different

(a) At 0.040 in thickness only
(b) At 18 ksi stress level only

These results are generally consistent with the Series IIIA results on the effect of stress; higher stresses decrease fatigue life and increase MSD. The fatigue life now increases monotonically with skin thickness although the difference between 0.063 and 0.080 inches cannot be declared as significant with just these test results. In any case, while an increase in fatigue life with increasing thickness is anticipated due to the diminishing of the knife edge, the increase is not nearly as large as that provided by the terminating action.

Part of the lower than expected increase in fatigue life with increasing skin thickness can be explained by the increase in bending associated with the thickest specimens (see Appendix E.) The 0.080 inch thick specimens have a measured bending stress just above the top row of rivets nearly equal to 15% of the maximum membrane stress. However, the bending stress for both the 0.040 and 0.063 inch thick specimens is approximately 5% to 7% of the maximum membrane stress. Nevertheless, these fatigue results suggest that the elimination of the knife edge through a use of thicker skin is not necessarily sufficient to greatly increase fatigue life.

The more detailed experiments of Series IIIB reinforce the result that increasing stress level does have a statistically significant effect on MSD. The average MSD for 20ksi corresponds to an equivalent of eight equal, 0.25 inch size cracks; the maximum MSD observed was 0.22 or the equivalent of 10 equal size cracks. Skin thickness is now observed to also have a significant effect on MSD, but the maximum is for the intermediate 0.063 inch value, while the minimum is for the largest thickness, 0.080 inches. No explanation for this phenomenon is evident.

Discussion

Lap Splice Simulation

One of the principal tasks of this project was the development of a flat test specimen that provides simulation of the mechanical conditions of a fuselage lap splice. The 12

inch wide, edge-reinforced panel does duplicate several characteristics of this detail: the membrane stress distribution, crack growth rates and MSD pattern are all very similar to all those found on B727 and B737 examples. A correlation to fatigue life is difficult to establish because of the few aircraft examples available and the uncertainty of when and to what degree bond integrity was lost in the fuselage lap splices. It certainly appears true that the fatigue lives of the 12 inch test panels are greater than those for actual fuselage lap splices; this is the case, on average, even without accounting for the number of cycles (flights) before failure of the lap splice bond or the variation in pressure differential with each flight. Nevertheless, it appears that the difference is not more than about a factor of two.

There may be several sources for this difference. Limited data from tests on unreinforced panels, see Figure 24, indicate that there may be a size effect on fatigue life. Aluminum sheets used to form fuselages are up to 216 inches (18ft) long. Perhaps the built-in stresses associated with fitting such large joints together causes a reduction in fatigue life.

Differences in bending between the test panels and a fuselage at the lap splice represents another possible source of the fatigue life discrepancy. A higher degree of bending in the fuselage could account for some reduction in fatigue life relative to the 12 inch test panels, but we are aware of no published measurements of this type. Calculations in [5] indicate that the local bending at a fuselage lap splice can be as high as 30-40% of the membrane stress. Bending in the 12 inch wide test panels ranged from 7-15% of the membrane stress, Appendix E. Other effects not simulated by the tests are: biaxial stress and environmental degradation.

Terminating Action

The increase in fatigue life associated with implementation of the terminating action was remarkable. The result of most practical importance is the four- to five-fold increase obtained after button head rivets are installed in crack free holes; this is the condition

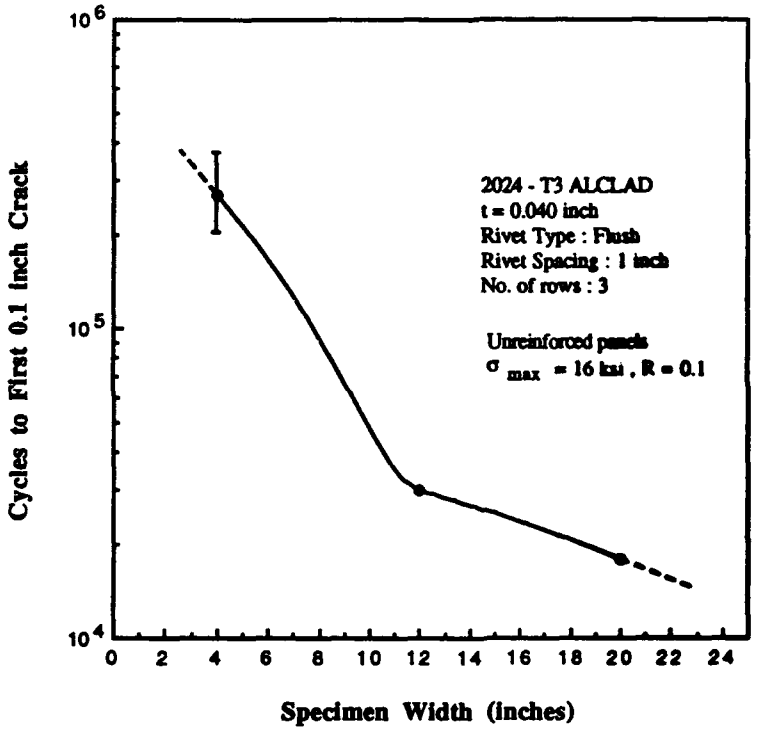

Figure 24: Data Suggesting that there is a Size Effect on Fatigue Life in Test Panels

strived for by the required repair. Most surprising was the substantial improvement in life obtained even in the presence of a crack that extended 0.1 inch beyond the edge of the rivet hole. Three explanations that have been raised to account for this phenomenon are:

1. reduction in bearing stress with the use of a larger diameter rivet; 0.219 vs. 0.156 inch,

2. crack retardation from overload of the crack tip during insertion of the button head rivet, and

3. load shedding due to increased friction between lapped sheets from the clamping force of the protruding head.

No experiments were performed to determine which of these or other effects, are responsible for the improvement, but the steady crack growth with number of cycles for at least one of the panels, Figure 13, suggests that there was no retardation in crack growth from a plastic zone. Also, while differences in bearing between rivet and hole may influence fatigue initiation, it seems unlikely that this would affect a crack tip which is 1.5 times the radius of the hole away from the edge. Therefore, the added clamping pressure appears to be the most likely explanation of high resistance to damage.

Shear

The addition of shear had, like the terminating action, a greater than expected effect on fatigue life. Experiments with shear were conducted to maintain a 16ksi maximum stress along the axis of the specimen. For a shear-to-tension ratio of 0.1, this results in a maximum nominal principal stress of 16.1ksi; strain gage results provided a value of approximately 16.4ksi. The fatigue life is roughly proportional to the inverse of the alternating stress raised to some power on the order of 4-6. If a power of 6 were used, one would expect a reduction in fatigue life with the addition of shear (0.1 ratio) of at most

$$(16.4/16)^6 - 1 = 0.16(16\%).$$

The observed average reduction, Figure 14, is approximately 33%. Of course, the calculation for fatigue life is more complicated than this, but it does appear that shear aggravates fatigue more than expected.

Lap Splice Parameters

A striking result of this study is that MSD can apparently occur in just about any type of lap splice configuration. Only the joints fabricated with Briles rivets failed to show regular MSD, but this is probably due to the very high fatigue lives associated with this construction and the consequent lack of any cracking.

The significant effect shown in this study that higher stresses cause greater MSD is consistent with current hypotheses of why MSD occurs in lap splices. Low scatter in fatigue lives at the individual rivet holes is one explanation for this phenomenon (c.f. [13]). It is certainly consistent with the low fatigue lives associated with MSD in fuselages and the fact that MSD is rarely perfectly uniform. The other explanation, which has the first as a necessary condition, is that small rivet hole cracks can "catch up" to larger ones due to an initially decreasing stress intensity factor with crack length (c.f. [14,15]. A physical basis for this effect - compressive residual stresses from the rivet shank - has been proposed by Beuth and Hutchinson [15]. It appears that the effect of stress on MSD is also consistent with this hypothesis, since crack growth rates increase with increasing nominal stress.

Effects of skin thickness on fatigue life and MSD have perhaps provided the most puzzling results. Detailed tests in Series IIIB showed that thickness has a significant effect on both of these parameters. However, the magnitude of the effect of increasing thickness on fatigue life is lower than expected as is its non-monotonic effect on MSD.

The reason for anticipating a large improvement in fatigue life with thickness is the

elimination of the knife edge. The knife edge is eliminated for the 0.063 and 0.080 inch thick sheet; Figure 25 shows a cross section for 0.080 inch skin. Nevertheless, the fatigue lives are increased less than a factor of two over that for the 0.040 inch thickness. Thus, elimination of the knife edge alone may not be sufficient to prevent the occurrence of MSD. Having stated this, it is necessary to explain the high fatigue lives of the Briles riveted panels, for which the knife edge is also eliminated. Perhaps the greater clamping pressure achieved with the 120° head on this rivet, like the flat underside of the button head rivets, provides the observed improvement.

Conclusions

- A 12 inch wide, edge-reinforced test panel provides reasonable simulation of the mechanical conditions of a fuselage lap splice.

- Membrane stress distribution, fatigue lives, crack growth rates and MSD patterns in this panel are all similar to those observed in limited examples from actual fuselages.

- The terminating action repair described in SB737-53-1039 is very effective in increasing fatigue life of lap splices, both under pure tension and combined shear and tension of the type expected at the window line of a fuselage.

- The terminating action is very effective even in the presence of cracks as large as 0.1 inch beyond the rivet hole, although such cracks should not escape detection in aircraft.

- The addition of small amounts of shear to the panels causes a substantial reduction in fatigue life relative to the pure tension results.

- Briles rivets impart a substantial improvement in fatigue life over flush head rivets.

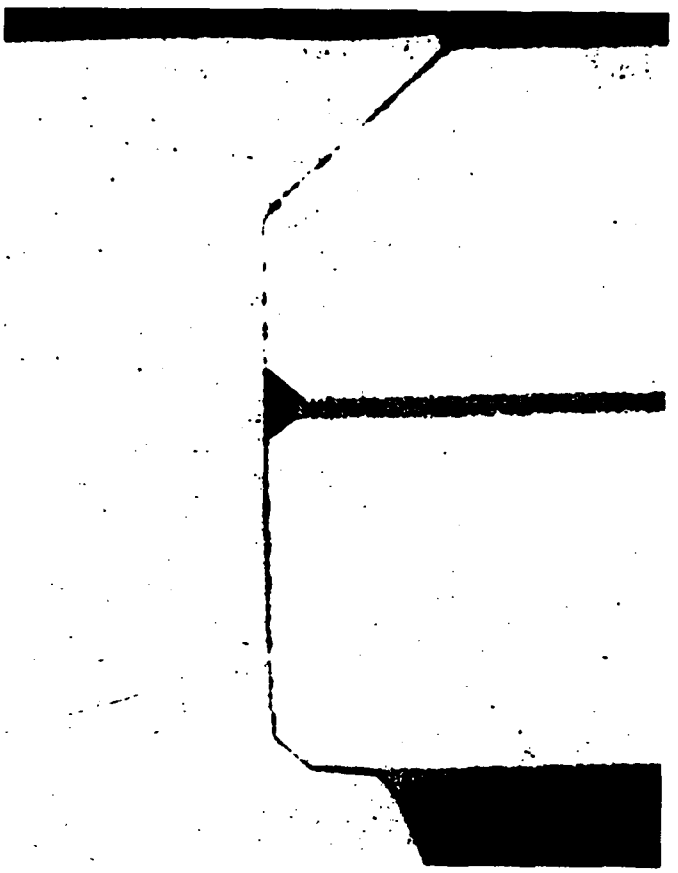

Figure 25: Cross Section of a Flush Head Rivet in 0.080 inch Thick Sheet

- Fatigue life is increased significantly with decreasing maximum stress.

- Increasing skin thickness increases fatigue life but by less than a factor of two in going from 0.040 to 0.080 inches.

- A measure was proposed to characterize the severity of MSD in test panels or fuselages.

- MSD occurred in every geometric lap splice configuration tested.

- MSD is increased significantly with increasing stress.

Acknowledgement

The authors would like to acknowledge the participation of several individuals and organizations in the performance of this project. Support was provided by the Federal Aviation Administration and monitored by the Volpe National Transportation Systems Center under contract DTRS-57-89-D-00007, Task VA9011. Technical monitors and technical participants included Drs. Kemal Arin and Sam Sampath, Mr. Jeffrey Gordon and Ms. Melanie Violette. Fatigue Technology, Inc., Seattle, WA with Richard Wagner provided testing and strain gaging support. Dr. Matthew Creager of Structural Integrity Engineering, Chatsworth, CA, provided guidance on aircraft design and analysis. Helio Precision Products, Bedford, MA fabricated the specimens. Special thanks go to Dr. Thomas Doerfler, statistics, Dr. Peter Hilton, review; Mr. Shaun Berry, testing; and Mr. William Wilson, strain gaging.

References

1. Aircraft Accident Report - Aloha Airlines, Flight 243, Boeing 737-200, N73711, Near Maui, Hawaii, April 28, 1988; National Transportation Safety Board Report NTSB/AAR-89/03 (June 14, 1989) 262 pages.

2. Boeing Service Bulletin No. 737-53-1039, Revision 2, Body Skin Lap Joint Inspection and Repair, Feb. 8, 1974 and Revision 3, August 20, 1987.

3. J. R. Maclin, "Performance of Fuselage Pressure Structure", presented at The third International Conference on Aging Aircraft and Structural Airworthiness, November 19-21, 1991, Washington, D.C.

4. Pelloux, R., Massachusetts Institute of Technology, Private Communication, 1991.

5. Samavedem, G. and Hoadley, D., "Fracture and Fatigue Strength Evaluation of MSC Damaged Aircraft Fuselages - Curved Panel Testing and Analysis," Report DTS-9024 to U.S. Dept. of transportation, Federal Aviation Administration. (May 1991) 157 pages.

6. Brock, D., "The Civil Damage Tolerance Requirements in Theory and Practice," in Structural Integrity of Aging Airplanes, S.N. Alturi, S.G. Sampath and P. Tong (Eds.) (Berlin; Springer-Verlag) 1991, Pages 73-86.

7. Mayville, R.A. and Warren, T.J., "A Laboratory Study of Fracture in the Presence of Lap Splice Multiple Site Damage", in Structural Integrity of Aging Airplanes, S.N. Atluri, S.G. Sampath and P. Tong (Eds.) (Berlin; Springer-Verlag) 1991.

8. Hahn, G.J. and S.S. Shapiro, "A Catalog and Computer Program for The Design and Analysis of Orthogonal Symmetric and Asymmetric Fractional Factorial Experiments", General Electric Report No. 66-C-165, May 1966.

9. Gunst, Richard F. and Mason, A.L., "How to Construct Fractional Factorial Experiments," American Society for Quality Control, Vol. 14, 1991.

10. Nelson, Wayne, Applied Life Data Analysis, John Wiley & Sons, (1982).

11. Snedecor, George and Cochran, W.G., Statistical Methods, Iowa State University Press, (1967).

12. SAS User's Guide: Statistics, SAS Institute, Cary, NC (1985).

13. Orringer, O., "How Likely is Multiple Site Damage," in Structural Integrity of Aging Airplanes, S.N. Atluri, S.G. Sampath and P. Tong (Eds.) (Berlin; Springer-Verlag) 1991, Pages 275-292.

14. deKoning, A.V., "MSDS: A Parameter Characterizing Structural Sensitivity for Multiple Site Damage Development," Memorandum SC-90-034, National Aerospace Laboratory NLR, the Netherlands (1990) 10 pages.

15. Beuth, Jr., J.L. and Hutchinson, J.W., "Preliminary Results on the Fracture Analysis of Multi-Cracking of Lap Joints in Aircraft Skins," Div. of Applied Sciences, Harvard University (December 1991) 20 pages.

APPENDIX A

MSD PATTERNS FROM SELECTED SPECIMENS

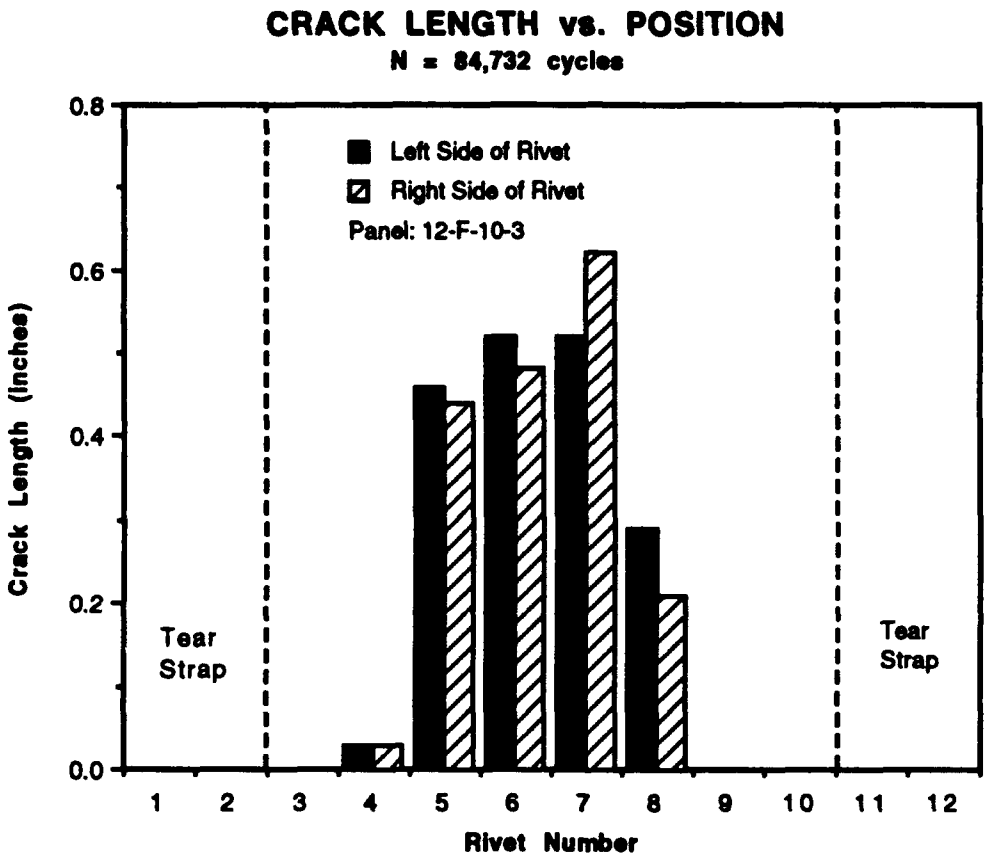
CRACK LENGTH vs. POSITION
N = 84,732 cycles
Left Side of Rivet
Right Side of Rivet
Panel: 12-F-10-3
Crack Length (inches)
0.0
0.2
0.4
0.6
0.8
Tear Strap
Tear Strap
1
2
3
4
5
6
7
8
9
10
11
12
Rivet Number

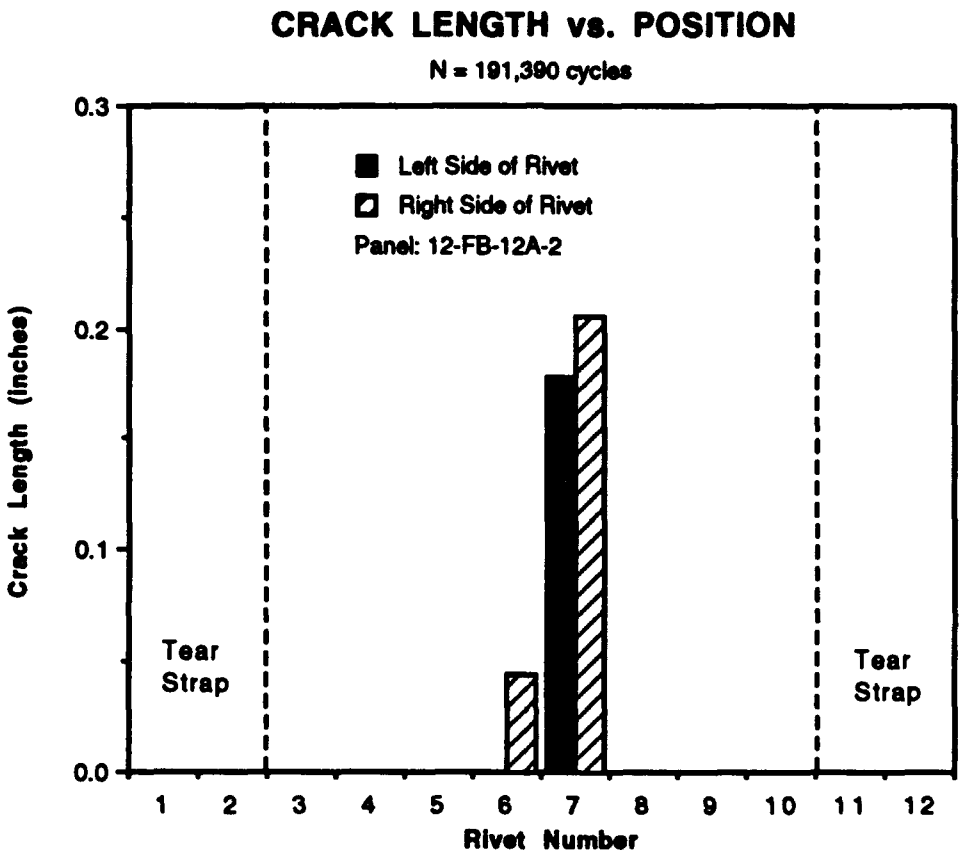
CRACK LENGTH vs. POSITION
N = 191,390 cycles
Left Side of Rivet
Right Side of Rivet
Panel: 12-FB-12A-2
Crack Length (inches)
0.3
0.2
0.1
0.0
Tear Strap
Tear Strap
1
2
3
4
5
6
7
8
9
10
11
12
Rivet Number

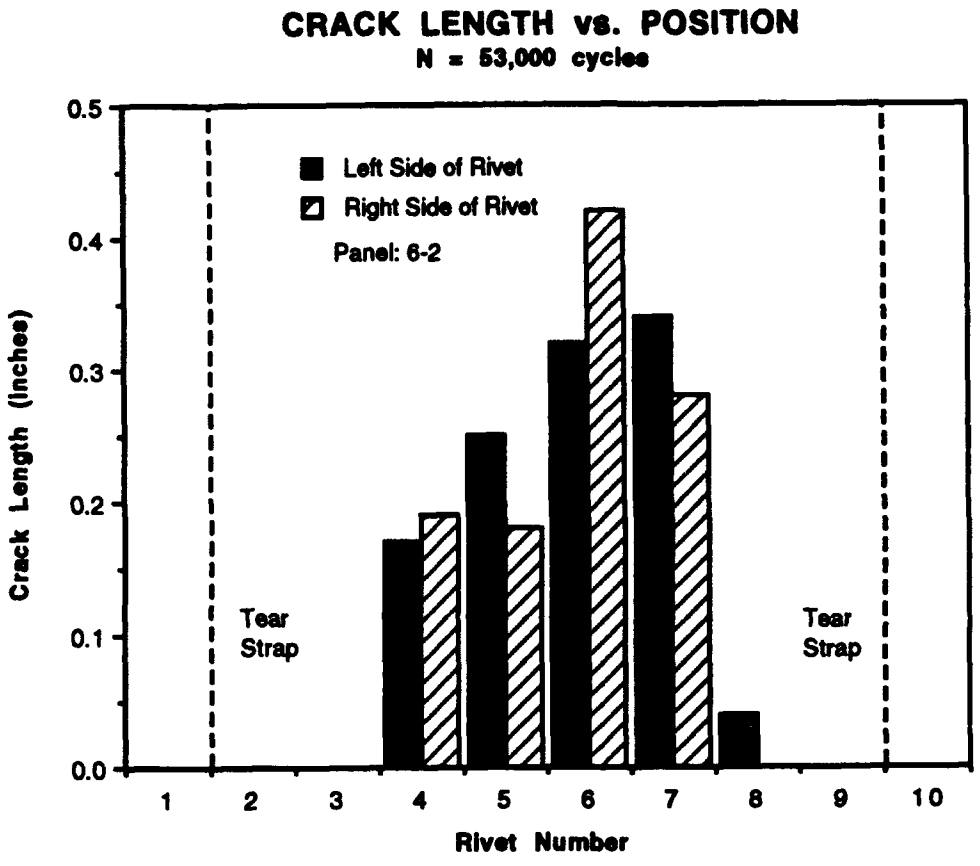
CRACK LENGTH vs. POSITION
N = 53,000 cycles
Left Side of Rivet
Right Side of Rivet
Panel: 6-2
Tear Strap
Tear Strap
Crack Length (Inches)
0.0
0.1
0.2
0.3
0.4
0.5
1
2
3
4
5
6
7
8
9
10
Rivet Number

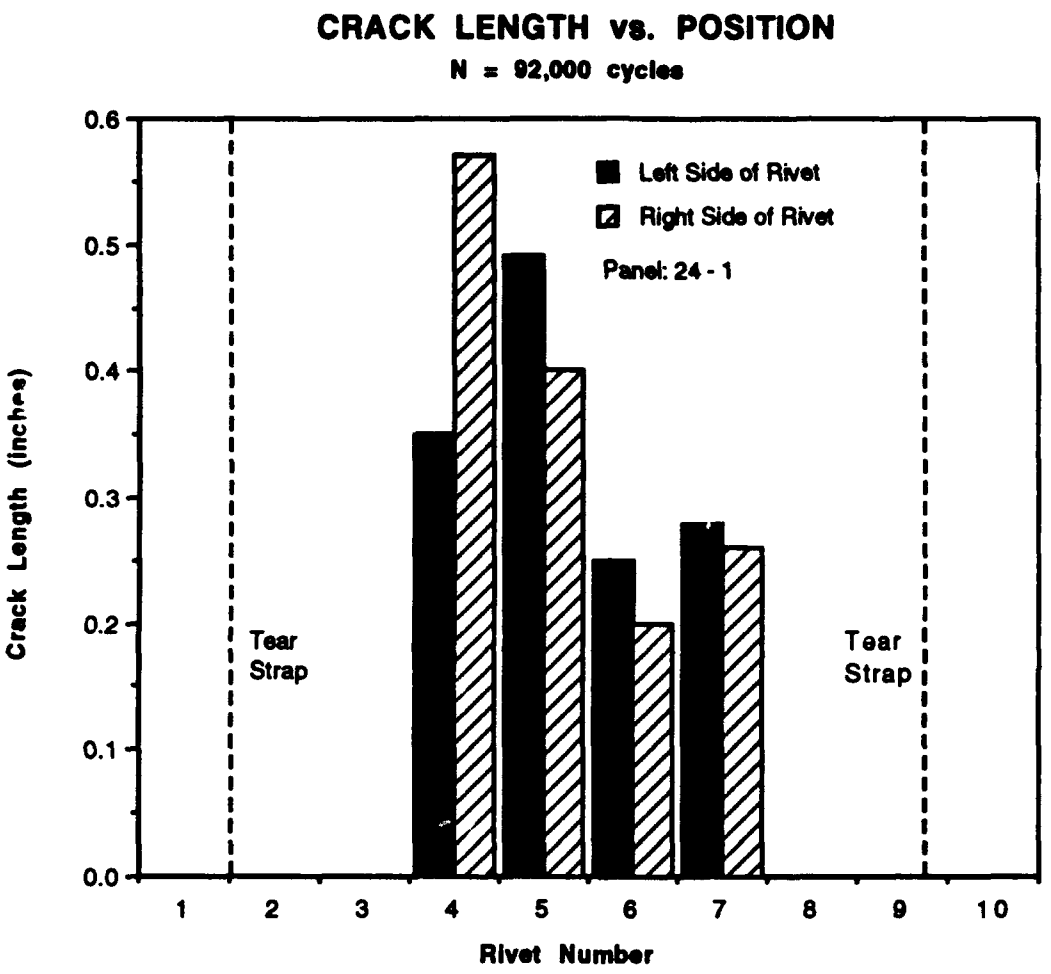
CRACK LENGTH vs. POSITION
N = 92,000 cycles
Left Side of Rivet
Right Side of Rivet
Panel: 24 - 1
Tear Strap
Tear Strap
Crack Length (inches)
0.0
0.1
0.2
0.3
0.4
0.5
0.6
1
2
3
4
5
6
7
8
9
10
Rivet Number

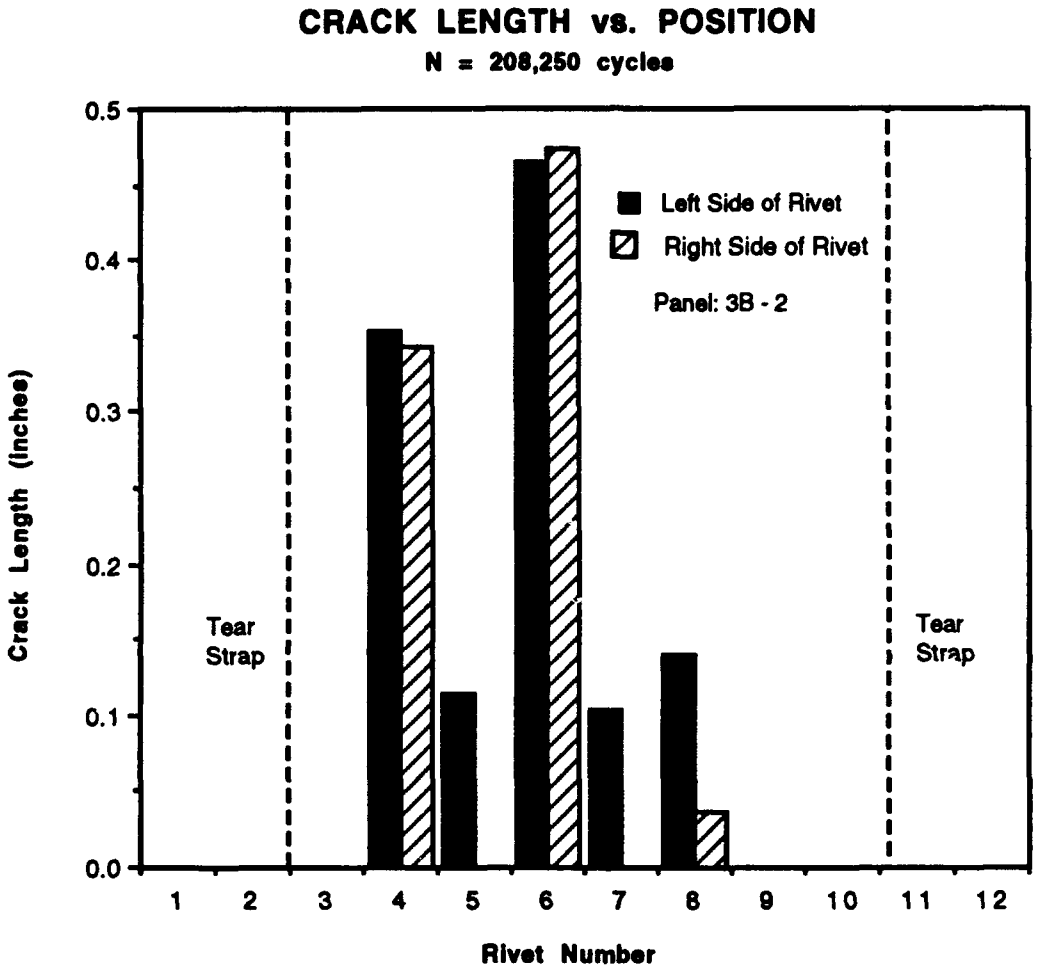
CRACK LENGTH vs. POSITION
N = 208,250 cycles
Crack Length (inches)
0.5
0.4
0.3
0.2
0.1
0.0
Tear Strap
Tear Strap
Left Side of Rivet
Right Side of Rivet
Panel: 3B - 2
1
2
3
4
5
6
7
8
9
10
11
12
Rivet Number

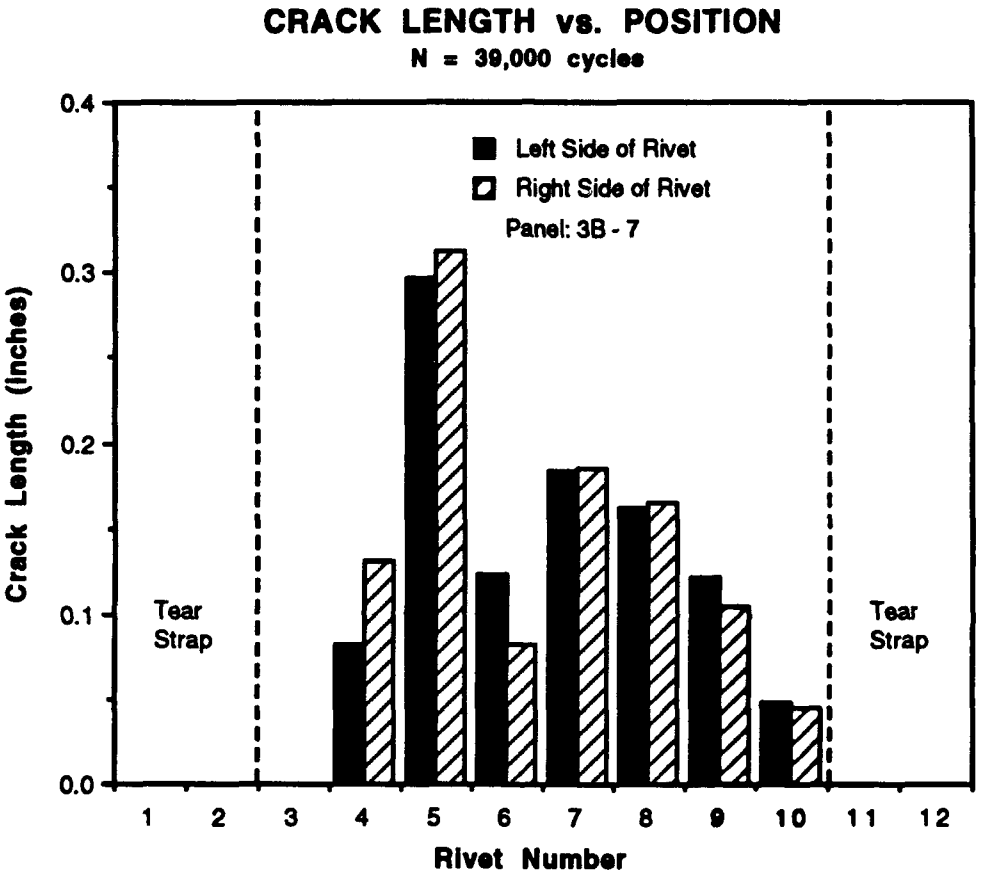
CRACK LENGTH vs. POSITION
N = 39,000 cycles
Left Side of Rivet
Right Side of Rivet
Panel: 3B - 7
Crack Length (Inches)
0.4
0.3
0.2
0.1
0.0
Tear Strap
Tear Strap
1
2
3
4
5
6
7
8
9
10
11
12
Rivet Number

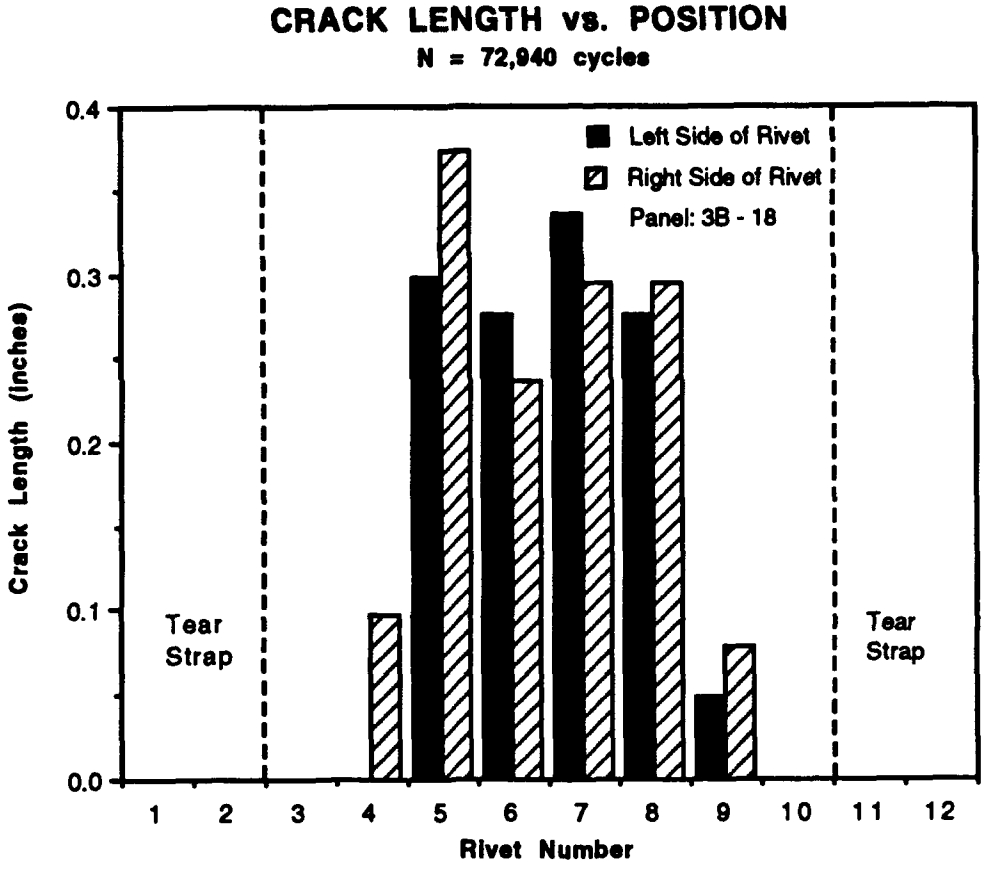
CRACK LENGTH vs. POSITION
N = 72,940 cycles
Left Side of Rivet
Right Side of Rivet
Panel: 3B - 18
Crack Length (inches)
0.4
0.3
0.2
0.1
0.0
Tear Strap
Tear Strap
1
2
3
4
5
6
7
8
9
10
11
12
Rivet Number

APPENDIX B

EXPERIMENTS TO DETERMINE THE EFFECT OF BUCKTAIL DIAMETER ON FATIGUE

Introduction

An experimental study was undertaken to determine the effect of bucktail diameter on fatigue life after a large difference was observed in 12 inch wide panel, baseline tests.

Test Design

The specimens geometry for this task consisted of a 4 inch wide, unreinforced lap splice specimen. All other parameters and test procedures were identical to those used for the 12 inch wide baseline tests described in the body of the report; for example, 0.040 inch skin thickness, flush head rivets, 16ksi maximum stress. The bucktail diameter was varied in fabrication to give approximately three different values: 0.235, 0.242 and 0.250 inches. All are within acceptable values but it is the upper value preferred in practice.

Results

The results of the tests are shown in Table B1 and Figure B1. Although there is scatter in the results, it is clear that fatigue life increases with bucktail diameter, over the range considered, and the maximum benefit is reached at intermediate diameters.

Table B1: Bucktail Diameter Test Results

Specimen	Bucktail Diameter (inches)	Cycles to First 0.1 inch Crack
4.BT1-1	0.235	89,809
4-BT1-2	0.233	42,973
4-BT1-3	0.234	115,284
4-BT2-1	0.250	256,718
4-BT2-2	0.254	283,442
4-BT2-3	0.245	315,250
4-BT3-2	0.241	207,163
4-BT3-3	0.241	316,328

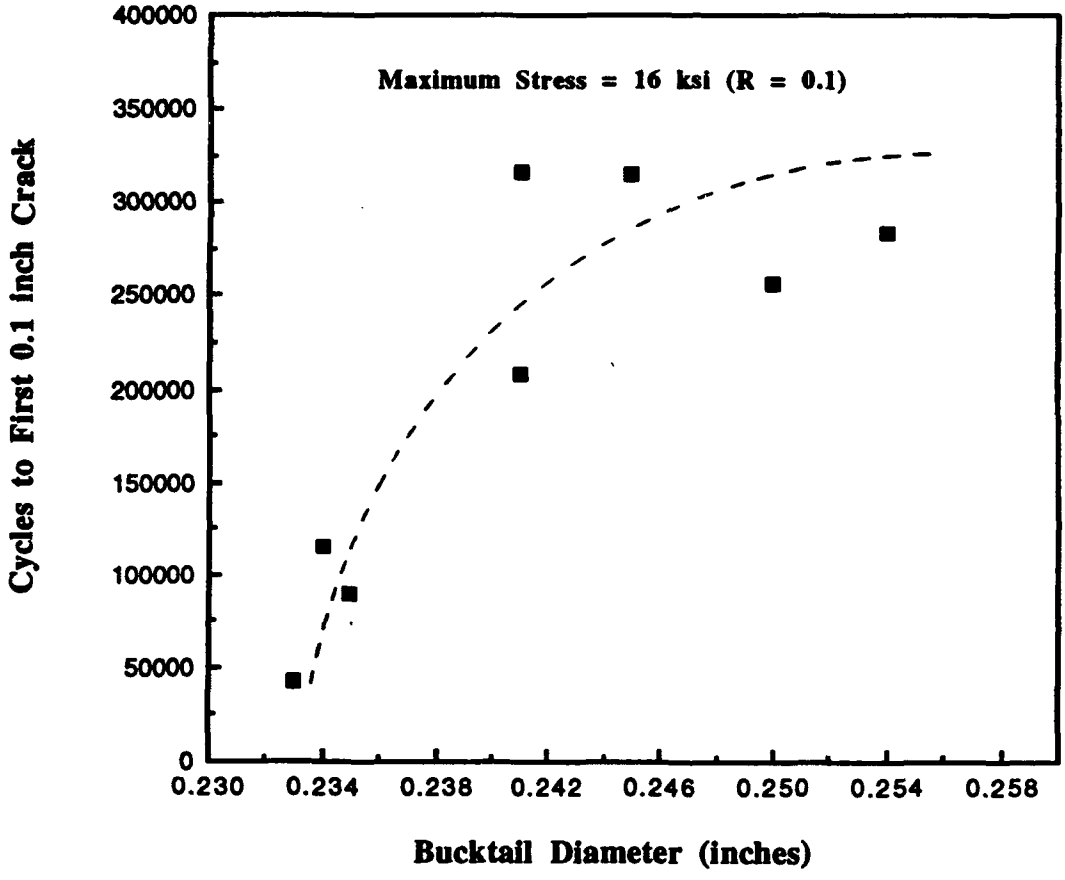

Figure B1: Effect of Bucktail Diameter on Fatigue Life

APPENDIX C

SERIES III TEST DATA

Series IIIA Test Matrix											
Test Number	Stress Level (ksi)	Rivet Type	Rivet Spacing (In)	Rivet Orientation	No. of Row	Skin Thickness (Inch)	Testing Loca-tion	Cycles to First 0.1 Inch Crack	Bucktail Diameter (in)	MSD	Total Cycles
1-2	12	Flush	1.0	Staggered	5	0.04	FTI	>668,705	.239	0	668,705
2-1	12	Briles	1.0	Staggered	3	0.05	FTI	>650,000	.243	0	650,000
3-2	12	Flush	1.0	Cont.	5	0.063	ADL	526,700	.240	0	526,700
4-1	12	Briles	1.29	Cont.	5	0.04	FTI	>506,000	.243	0	506,000
5-2	12	Flush	1.29	Staggered	5	0.05	ADL	175,766	.240	0.016	307,650
6-1	12	Flush	1.29	Staggered	3	0.063	FTI	175,000	.243	0.020	230,000
7-2	12	Flush	0.75	Staggered	3	0.04	ADL	>400,000	.240	0	400,000
8-1	12	Flush	0.75	Cont.	5	0.05	FTI	350,000	.241	0.022	462,000
9-1	12	Briles	0.75	Staggered	5	0.063	FTI	>800,000	.241	0	800,000
10-1	14	Briles	1.0	Cont.	3	0.04	ADL	-	.241	-	-
10-2	14	Briles	1.0	Cont.	3	0.04	ADL	>296,000	.243	0	295,340
11-1	14	Flush	1.0	Staggered	5	0.05	FTI	134,000	.241	0.044	206,000
11-2	14	Flush	1.0	Staggered	5	0.05	FTI	134,000	.241	0.032	200,000
12-1	14	Flush	1.0	Staggered	5	0.063	FTI	196,000	.241	0.026	240,000
12-2	14	Flush	1.0	Staggered	5	0.063	FTI	256,000	.242	0.035	296,000
13-1	14	Flush	1.29	Staggered	5	0.04	FTI	442,000	.239	0.027	570,000
13-2	14	Flush	1.29	Staggered	5	0.04	FTI	294,000	.241	0.014	518,000
14-1	14	Flush	1.29	Cont.	3	0.05	FTI	68,000	.243	0.028	116,000
14-2	14	Flush	1.29	Cont.	3	0.05	FTI	95,000	.243	0.018	165,000
15-1	14	Briles	1.29	Staggered	5	0.063	ADL	>400,000	.243	0	400,000

Series IIIA Test Matrix											
Test Number	Stress Level (ksi)	Rivet Type	Rivet Spacing (In)	Rivet Orientation	No. of Row	Skin Thickness (Inch)	Testing Loca-tion	Cycles to First 0.1 Inch Crack	Bucktail Diameter (in)	MSD	Total Cycles
15-2	14	Briles	1.29	Staggered	5	0.063	ADL	348,020	.242	0	348,020
16-1	14	Flush	0.75	Staggered	5	0.04	FTI	>440,000	.240	0	440,000
16-2	14	Flush	0.75	Staggered	5	0.04	FTI	>400,000	.240	0	400,000
17-1	14	Briles	0.75	Staggered	5	0.05	ADL	>379,200	.242	0	379,200
17-2	14	Briles	0.75	Staggered	5	0.05	ADL	>291,360	.243	0	291,360
18-1	14	Flush	0.75	Cont.	3	0.063	FTI	162,000	.241	0.069	198,000
18-2	14	Flush	0.75	Cont.	3	0.063	FTI	226,000	.242	0.028	266,000
19-1	16	Flush	1.0	Staggered	5	0.04	FTI	182,000	.240	0.057	286,000
19-2	16	Flush	1.0	Staggered	5	0.04	FIT	354,000	.240	0.044	420,000
20-1	16	Flush	1.0	Cont.	5	0.05	ADL	66,000	.242	0.033	99,640
20-2	16	Flush	1.0	Cont.	5	0.05	ADL	54,000	.240	0.028	79,000
21-1	16	Briles	1.0	Staggered	3	0.063	FTI	137,000	.242	0.042	164,000
21-2	16	Briles	1.0	Staggered	3	0.063	FTI	98,000	.241	0.056	122,000
22-1	16	Flush	1.29	Staggered	3	0.04	ADL	88,000	.241	0.025	121,750
22-2	16	Flush	1.29	Staggered	3	0.04	ADL	148,000	.239	0.041	170,950
23-1	16	Briles	1.29	Staggered	5	0.05	FTI	>206,000	.242	0	206,000
23-2	16	Briles	1.29	Staggered	5	0.05	FTI	>162,242	.242	0	162,000
24-1	16	Flush	1.29	Cont.	5	0.063	FTI	65,000	.239	0.078	92,000
24-2	16	Flush	1.29	Cont.	5	0.063	FTI	78,000	.242	0.014	118,000
25-1	16	Briles	0.75	Cont.	5	0.04	FTI	>211,650	.243	0	211,650
25-2	16	Briles	0.75	Cont.	5	0.04	FTI	>194,000	.243	0	194,000

Series IIIA Test Matrix											
Test Number	Stress Level (ksi)	Rivet Type	Rivet Spacing (In)	Rivet Orientation	No. of Row	Skin Thickness (Inch)	Testing Loca-tion	Cycles to First 0.1 Inch Crack	Bucktail Diameter (in)	MSD	Total Cycles
26-1	16	Flush	0.75	Staggered	3	0.05	FTI	90,000	.241	0.088	100,000
26-2	16	Flush	0.75	Staggered	3	0.05	FTI	70,000	.243	0.040	96,000
27-1	16	Flush	0.75	Staggered	5	0.063	ADL	289,560	.241	0	289,560
27-2	16	Flush	0.75	Staggered	5	0.063	ADL	127,846	.243	0.039	168,970
1-1	18	Flush	1.0	Staggered	5	0.04	FTI	120,000	.238	0.047	190,000
2-2	18	Briles	1.0	Staggered	3	0.05	FTI	>134,000	.243	0	134,000
4-2	18	Briles	1.29	Cont.	5	0.04	FTI	>143,000	.242	0	143,000
6-2	18	Flush	1.29	Staggered	3	0.063	FTI	38,000	.243	0.098	53,000
8-2	18	Flush	0.75	Cont.	5	0.05	FTI	125,000	.242	0.046	141,000
9-2	18	Briles	0.75	Staggered	5	0.063	FTI	268,000	.241	0.031	290,000
*3-1	27	Flush	1.0	Cont.	5	0.063	ADL	14,706	.241	-	17,170
*5-1	27	Flush	1.29	Staggered	5	0.05	ADL	<12,700	.242	-	13,600
*7-1	27	Flush	0.75	Staggered	3	0.04	ADL	26,000	.239	-	27,730

*Panel erroneously tested at 27 KSI

Distribution Of Cracks For Series IIIA Test Panels																	
Panel I.D.	Rivet Number (number of cracks per rivet)															No. of Cracked Holes	Total Cycles
	1	2	3	4	5	6	7	8	9	10	11	12	13	14	15		
1-2																0	668,705
2-1																0	650,000
3-2					1	1										2	526,700
4-1																0	506,000
5-2					1		2									2	307,650
6-1					2	2	2									3	230,000
7-2																0	400,000
8-1					1	1	2									3	462,000
9-1																0	800,000
10-1																0	400,000
10-2																0	295,340
11-1				2					2	1						3	206,000
11-2					2			2	2							3	200,000
12-1					2											1	240,000
12-2						2	1		2							3	296,000
13-1		1							2							2	570,000
13-2									1	1						2	518,000
14-1				2	2	2										3	116,000

Distribution Of Cracks For Series IIIA Test Panels																	
Panel I.D.	Rivet Number (number of cracks per rivet)															No. of Cracked Holes	Total Cycles
	1	2	3	4	5	6	7	8	9	10	11	12	13	14	15		
14-2				2	2	2	1									4	160,000
15-1																0	400,000
15-2																0	348,000
16-1																0	440,000
16-2																0	400,000
17-1																0	379,000
17-2																0	291,361
18-1				1	2	2			1	2						5	198,000
18-2						2		2								2	266,000
19-1	2										2					2	286,000
19-2	1	1									2	2				4	420,000
20-1					2		1									2	99,640
20-2					1	2	2									3	79,000
21-1						1	2	2								3	164,000
21-2				1	2	2	2	2	1							6	122,000
22-1						2	1		1							3	121,000
22-2				1	2	2	2									4	170,950
23-1																0	206,000
23-2																0	162,000

Distribution Of Cracks For Series IIIA Test Panels																	
Panel I.D.	Rivet Number (number of cracks per rivet)															No. of Cracked Holes	Total Cycles
	1	2	3	4	5	6	7	8	9	10	11	12	13	14	15		
24-1				2	2	2	2									4	92,000
24-2					2											1	118,000
25-1																0	211,650
25-2																0	194,000
26-1									2	2	2					3	100,000
26-2								2	2							2	96,000
27-1		2														1	289,560
27-2								2		2						2	168,000
1-1											2	2				2	190,000
2-2																0	134,000
4-2																0	143,000
6-2				2	2	2	2									4	53,000
8-2										1	1			1		3	141,000
9-2								2	1							2	290,000
*3-1					2		2		1							3	17,170
*5-1				2	1	2	2									4	13,600
*7-1						2	2									2	27,730

* Panels erroneously tested at 27 KSI

Aging Aircraft Study
Full Model - 27 obs - Bal

General Linear Models Procedure

Dependent Variable: LCYCLES

Source	DF	Sum of Squares	Mean Square	F Value	Pr > F
Model	22	3.61262283	0.16421013	3.64	0.1088
Error	4	0.18035154	0.04508789		
Corrected Total	26	3.79297437			

R-Square	C.V.	Root MSE	LCYCLES Mean
0.952451	3.888773	0.21233908	5.46031108

Source	DF	Type I SS	Mean Square	F Value	Pr > F
STRESS	2	1.48937732	0.74468866	16.52	0.0117
RIVTYPE	1	0.82889497	0.82889497	18.38	0.0128
RIVSPACE	2	0.20467313	0.10233656	2.27	0.2194
RORIENT	1	0.10501240	0.10501240	2.33	0.2017
NUMROWS	1	0.16407142	0.16407142	3.64	0.1291
SKINTHK	2	0.55915584	0.27957792	6.20	0.0595
TESTLOC	1	0.00105444	0.00105444	0.02	0.8859
STRESS*RIVSPACE	4	0.17693779	0.04423445	0.98	0.5072
STRESS*SKINTHK	4	0.01613210	0.00403302	0.09	0.9809
RIVSPACE*SKINTHK	4	0.06731341	0.01682835	0.37	0.8185

Source	DF	Type III SS	Mean Square	F Value	Pr > F
STRESS	2	1.48937732	0.74468866	16.52	0.0117
RIVTYPE	1	0.82889497	0.82889497	18.38	0.0128
RIVSPACE	2	0.20467313	0.10233656	2.27	0.2194
RORIENT	1	0.10501240	0.10501240	2.33	0.2017
NUMROWS	1	0.16407142	0.16407142	3.64	0.1291
SKINTHK	2	0.55915584	0.27957792	6.20	0.0595
TESTLOC	1	0.00105444	0.00105444	0.02	0.8859
STRESS*RIVSPACE	4	0.17693779	0.04423445	0.98	0.5072
STRESS*SKINTHK	4	0.01613210	0.00403302	0.09	0.9809
RIVSPACE*SKINTHK	4	0.06731341	0.01682835	0.37	0.8185

Parameter		Estimate	T for H0: Parameter=0	Pr > |T|	Std Error of Estimate
INTERCEPT		5.005301000 B	26.73	0.0001	0.18726547
STRESS	12	0.376160606 B	1.68	0.1681	0.22382504
	14	0.289088369 B	1.29	0.2661	0.22382504
	16	0.000000000 B	.	.	.
RIVTYPE	Briles	0.371684223 B	4.29	0.0128	0.08668707

Series IIIB Test Results

Specimen	Stress (ksi)	Thickness (inch)	Cycles to First 0.1 inch Crack	MSD
3B-1	14	0.040	93,609	0.024
3B-2	14	0.040	149,559	0.054
3B-3	14	0.040	109,161	0.052
3B-4	18	0.040	42,834	0.124
3B-5	18	0.040	57,408	0.120
3B-6	18	0.040	48,316	0.105
3B-7	20	0.040	30,333	0.216
3B-8	20	0.040	23,973	0.152
3B-9	20	0.040	29,058	0.079
3B-10	14	0.040	110,351	0.045
3B-11	14	0.040	88,482	0.039
3B-12	18	0.063	54,200	0.129
3B-13	18	0.080	78,558	0.078
3B-14	18	0.063	63,190	0.140
3B-15	18	0.080	59,882	0.037
3B-17	18	0.080	66,369	0.042
3b-18	18	0.063	61,796	0.171
3B-21	18	0.080	111,849	0.045
3B-22	18	0.040	46,162	0.086
3B-23	18	0.040	52,857	0.098
3B-24	18	0.040	29,252	0.154

Aging Aircraft Study
Added Tests

OBS	TESTNUM	STRESS	SKINTHK	MSD	RIVTYPE	CYCLES	LCYCLES	SQRTMSD
1	B-01	14	0.040	0.024	F	93609	4.97132	0.15492
2	B-02	14	0.040	0.054	F	149559	5.17481	0.23238
3	B-03	14	0.040	0.052	F	109161	5.03807	0.22804
4	B-04	18	0.040	0.124	F	42834	4.63179	0.35214
5	B-05	18	0.040	0.120	F	57408	4.75897	0.34641
6	B-06	18	0.040	0.105	F	48316	4.68409	0.32404
7	B-07	20	0.040	0.216	F	30333	4.48192	0.46476
8	B-08	20	0.040	0.125	F	23973	4.37972	0.35355
9	B-09	20	0.040	0.079	F	29058	4.46327	0.28107
10	B-10	14	0.040	0.045	F	116351	5.06577	0.21213
11	B-11	14	0.040	0.039	F	88482	4.94685	0.19748
12	B-12	18	0.063	0.129	F	54200	4.73400	0.35917
13	B-13	18	0.080	0.078	F	78558	4.89519	0.27928
14	B-14	18	0.063	0.140	F	63190	4.80065	0.37417
15	B-15	18	0.080	0.037	F	59882	4.77730	0.19235
16	B-17	18	0.080	0.042	F	66369	4.82197	0.20494
17	B-18	18	0.063	0.171	F	61796	4.79096	0.41352
18	B-21	18	0.080	0.045	F	111849	5.04863	0.21213
19	B-22	18	0.040	0.086	F	46162	4.66428	0.29326
20	B-23	18	0.040	0.098	F	52857	4.72310	0.31305
21	B-24	20	0.040	0.154	F	29252	4.46616	0.39243

Aging Aircraft Study
Added Tests - ANOVA - skin thickness = .04 only

General Linear Models Procedure

Dependent Variable: MSD

Source	DF	Sum of Squares	Mean Square	F Value	Pr > F
Model	2	0.02370021	0.01185011	11.40	0.0021
Error	11	0.01143500	0.00103955		
Corrected Total	13	0.03513521			

R-Square	C.V.	Root MSE	MSD Mean
0.674543	34.17016	0.03224198	0.09435714

Source	DF	Type III SS	Mean Square	F Value	Pr > F
STRESS	2	0.02370021	0.01185011	11.40	0.0021

Parameter		Estimate	T for H0: Parameter=0	Pr > |T|	Std Error of Estimate
INTERCEPT		0.1435000000 B	8.90	0.0001	0.01612099
STRESS	14	-.1007000000 B	-4.66	0.0007	0.02162858
	18	-.0369000000 B	-1.71	0.1160	0.02162858
	20	0.0000000000 B	.	.	.

NOTE: The X'X matrix has been found to be singular and a generalized inverse was used to solve the normal equations. Estimates followed by the letter 'B' are biased, and are not unique estimators of the parameters.

Observation	Observed Value	Predicted Value	Residual	Lower 95% CL for Mean	Upper 95% CL for Mean
1	0.02400000	0.04280000	-0.01880000	0.01106376	0.07453624
2	0.05400000	0.04280000	0.01120000	0.01106376	0.07453624
3	0.05200000	0.04280000	0.00920000	0.01106376	0.07453624
4	0.12400000	0.10660000	0.01740000	0.07486376	0.13833624
5	0.12000000	0.10660000	0.01340000	0.07486376	0.13833624
6	0.10500000	0.10660000	-0.00160000	0.07486376	0.13833624
7	0.21600000	0.14350000	0.07250000	0.10801780	0.17898220
8	0.12500000	0.14350000	-0.01850000	0.10801780	0.17898220
9	0.07900000	0.14350000	-0.06450000	0.10801780	0.17898220
10	0.04500000	0.04280000	0.00220000	0.01106376	0.07453624
11	0.03900000	0.04280000	-0.00380000	0.01106376	0.07453624
12	0.08600000	0.10660000	-0.02060000	0.07486376	0.13833624
13	0.09800000	0.10660000	-0.00860000	0.07486376	0.13833624
14	0.15400000	0.14350000	0.01050000	0.10801780	0.17898220

Aging Aircraft Study
Added Tests - ANOVA - 18ksi only

General Linear Models Procedure

Dependent Variable: MSD

Source	DF	Sum of Squares	Mean Square	F Value	Pr > F
Model	2	0.01650005	0.00825002	24.98	0.0002
Error	9	0.00297287	0.00033032		
Corrected Total	11	0.01947292			

R-Square	C.V.	Root MSE	MSD Mean
0.847333	18.56136	0.01817467	0.09791667

Source	DF	Type III SS	Mean Square	F Value	Pr > F
SKINTHK	2	0.01650005	0.00825002	24.98	0.0002

Parameter		Estimate	T for H0: Parameter=0	Pr > |T|	Std Error of Estimate
INTERCEPT		0.0505000000 B	5.56	0.0004	0.00908733
SKINTHK	0.04	0.0561000000 B	4.60	0.0013	0.01219194
	0.063	0.0961666667 B	6.93	0.0001	0.01388113
	0.08	0.0000000000 B	.	.	.

NOTE: The X'X matrix has been found to be singular and a generalized inverse was used to solve the normal equations. Estimates followed by the letter 'B' are biased, and are not unique estimators of the parameters.

Observation	Observed Value	Predicted Value	Residual	Lower 95% CL for Mean	Upper 95% CL for Mean
1	0.12400000	0.10660000	0.01740000	0.08821312	0.12498688
2	0.12000000	0.10660000	0.01340000	0.08821312	0.12498688
3	0.10500000	0.10660000	-0.00160000	0.08821312	0.12498688
4	0.12900000	0.14666667	-0.01766667	0.12292931	0.17040402
5	0.07800000	0.05050000	0.02750000	0.02994285	0.07105715
6	0.14000000	0.14666667	-0.00666667	0.12292931	0.17040402
7	0.03700000	0.05050000	-0.01350000	0.02994285	0.07105715
8	0.04200000	0.05050000	-0.00850000	0.02994285	0.07105715
9	0.17100000	0.14666667	0.02433333	0.12292931	0.17040402
10	0.04500000	0.05050000	-0.00550000	0.02994285	0.07105715
11	0.08600000	0.10660000	-0.02060000	0.08821312	0.12498688
12	0.09800000	0.10660000	-0.00860000	0.08821312	0.12498688

APPENDIX D

DEFINITION OF MSD

Proposed Measures for MSD

A measure for MSD was needed to perform a statistical analysis on Series III testing. The following measure is proposed:

$$MSD = \left(\frac{W'}{\Sigma l_i} - 1\right) / \left(\frac{\sigma_f}{\sigma_n}\frac{W'}{W} - 1\right); \; evaluated \; at \; a_{max} = 0.25 \; inch \qquad (1)$$

where W = width of the specimen

$W' = W - nd_{rivet}$

n = number of rivets in the top row

d_{rivet} = diameter of the rivet head

Σl_i = sum of the remaining ligaments lengths at $N=N_O$

a_{max} = length of maximum size crack

σ_f = flow strength of the aluminum (average of yield and tensile strengths)

σ_n = nominal stress applied in the test

This equation was derived from the following net section "yielding" failure criterion:

$$\sigma_f \cdot \Sigma l_i \cdot t = \sigma_n \cdot W \cdot t \qquad (2)$$

where t is the skin thickness. The precise form of Equation (1) was chosen so that MSD = 0 when there are no cracks, $\Sigma l_i = W'$, and MSD = 1 when fracture is predicted by Equation (2); that is when:

$$\Sigma l_i = \frac{\sigma_n}{\sigma_f} W$$

Equation (2) has been validated for the case in which every rivet has two cracks all of equal size or $l_1 = l_2 = l_3 = ...$ (see [7] of the main report). It is only an approximation for unequal crack sizes; additional research would be required to improve Equation (2) for the general case.

The benefit of equation (1) is that it includes the risk of fracture, which is different for different nominal stress levels. The equation is evaluated when the first crack reaches a size of 0.25 inches, because the worse situation would be when all cracks were the same size equal to the critical crack size, which is approximately 0.25 inches.

Figure D1 shows an example plot of MSD vs. number of equal size cracks for the baseline specimen configuration.

As a comparison, the value of MSD for the central section of the B727 example shown in Figure 4 in the body of the report is approximately 0.24; a 16ksi nominal stress was assumed.

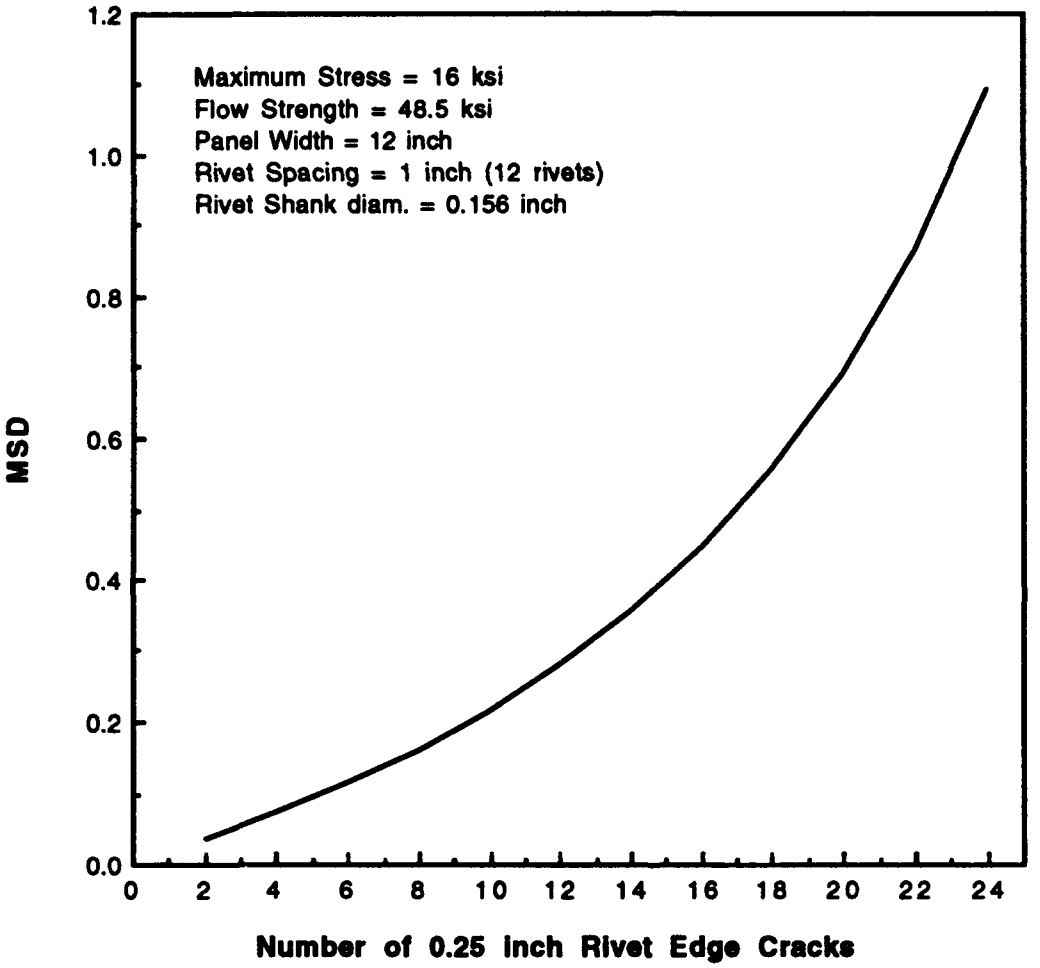

Figure D1: Relationship Between Number of Cracks and MSD According to the Definition (1)

APPENDIX E

STRAIN GAGE TESTS ON BENDING IN 12 INCH WIDE PANELS

Bending Tests

A set of experiments was performed to estimate the degree of bending that occurs in the 12 inch wide, edge-reinforced panels for various thicknesses. Strain gages were applied to one panel of each of three thicknesses - 0.040, 0.063 and 0.080 inches. The gages were oriented axially, located 1 inch above the centerline of the top row and 1 inch below the bottom row on both sides of the specimen. Readings of strain were made for various levels of membrane stress.

The results are plotted in Figure E1 as the ratio of bending stress-to-membrane stress vs. membrane stress. The definitions of these two values is:

$$\sigma_m = (\sigma_{front} + \sigma_{rear})/2$$

$$\sigma_b = (\sigma_{front} \sigma_{rear})/2.$$

Data from the top gages is of greatest interest, since these are closest to the top row of rivets at which fatigue initiates. The figure shows that the bending stress decreases as a percentage of membrane stress as the membrane stress increases. l At σ_m = 16ksi, the bending stress ranges from 5-15% of the membrane stress. The 0.040 and 0.063 inch thick specimens had the lowest degree of bending, while the 0.080 inch thick specimen had bending of 15% of the membrane stress.

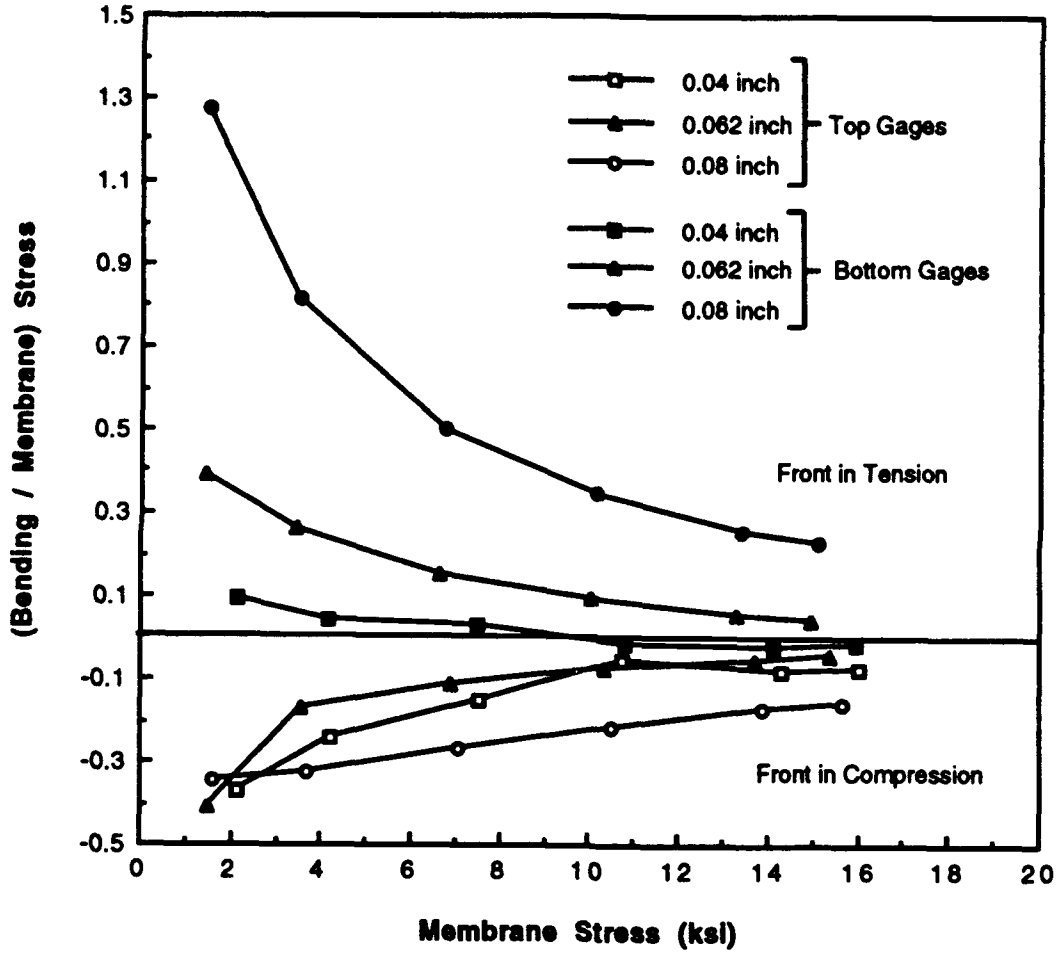

Figure E1: Relative Bending Stresses in the 12 Inch Wide Panels for Various skin Thicknesses